© 2023. Published by The Company of Biologists Ltd | Development (2023) 150, dev201297. doi:10.1242/dev.201297

RESEARCH ARTICLE

Stuxnet fine-tunes *Notch* dose during development using a functional Polycomb response element

Tao He[1,2,*], Yu Fan[1,*], Juan Du[3], Mengyuan Yi[1], Yajuan Li[1], Min Liu[1,2,‡] and Alan Jian Zhu[1,2,‡]

ABSTRACT

Evolutionarily conserved Notch signaling is highly sensitive to changes in Notch receptor dose caused by intrinsic and environmental fluctuations. It is well known that epigenetic regulation responds dynamically to genetic, cellular and environmental stresses. However, it is unclear whether the Notch receptor dose is directly regulated at the epigenetic level. Here, by studying the role of the upstream epigenetic regulator Stuxnet (Stx) in *Drosophila* developmental signaling, we find that Stx promotes *Notch* receptor mRNA expression by counteracting the activity of Polycomb repressive complex 1 (PRC1). In addition, we provide evidence that *Notch* is a direct PRC1 target by identifying and validating *in vivo* the only bona fide Polycomb response element (PRE) among the seven Polycomb group (PcG)-binding sites revealed by DamID-seq and ChIP-seq analysis. Importantly, *in situ* deletion of this PRE results in increased *Notch* expression and phenotypes resembling *Notch* hyperactivation in cell fate specification. These results not only underscore the importance of epigenetic regulation in fine-tuning the Notch activity dose, but also the need to assess the physiological significance of omics-based PcG binding in development.

KEY WORDS: Epigenetic regulation, *Notch*, PRC1, PRE, Stuxnet

INTRODUCTION

Notch signaling is evolutionarily conserved, and it controls many important biological processes in metazoan development and adult homeostasis (Henrique and Schweisguth, 2019; Sprinzak and Blacklow, 2021). Dysfunction of Notch signaling often leads to birth defects and cancer in humans (Aster et al., 2017; Mašek and Andersson, 2017; McIntyre et al., 2020). Activation of Notch signaling depends on the proteolytic cleavage and direct translocation of the intracellular domain of the Notch receptor (N^{icd}) into the nucleus, where N^{icd} binds to transcription factor Suppressor of Hairless [Su(H)] and activates the expression of downstream target genes. Notch signaling activation is dose sensitive to Notch receptors due to direct signaling from the plasma membrane to the nucleus. In *Drosophila*, heterozygotes carrying one copy of the loss-of-function *Notch* mutation show a stereotypical notched wing phenotype, whereas females harboring three copies of the *Notch* gene display the *Confluens* wing vein phenotype (Artavanis-Tsakonas and Muskavitch, 2010). Similarly, Notch receptor haploinsufficiency and increased *Notch* gene copy number in mammals are associated with multiple forms of developmental anomalies and cancer (Aster et al., 2017; Mašek and Andersson, 2017). Therefore, the dose of Notch receptors must be tightly controlled to ensure normal development and adult tissue homeostasis.

Modulation of Notch receptor dose occurs at multiple levels. At the transcriptional level, a few transcription factors and co-factors have been shown to bind directly to the *Notch* loci and control their transcription (Lambertini et al., 2010; Lefort et al., 2007; Koyama et al., 2014; Taranova et al., 2006; Wang et al., 2019; Wu et al., 2005). At the protein level, several E3 ligases (Hori et al., 2004; Jehn et al., 2002; Mukherjee et al., 2005; Qiu et al., 2000; Sakata et al., 2004; Wilkin et al., 2004) and γ-secretases (Cras-Méneur et al., 2009; De Strooper et al., 1999; Struhl and Greenwald, 1999; Wu et al., 2001) have been shown to mediate the ubiquitylation and processing of Notch receptors, thereby regulating their stability or signaling activity. Ubiquitylation-mediated degradation of Notch receptors can be further regulated by other forms of post-translational modifications, including phosphorylation, acetylation and methylation (Foltz et al., 2002; Fryer et al., 2004; Guarani et al., 2011; Hein et al., 2015; Li et al., 2014; Mo et al., 2007; Sjöqvist et al., 2014). Furthermore, O-fucosyltransferase 1 (O-fut1) interacts with the extracellular domain of Notch to facilitate its endocytosis and turnover (Sasamura et al., 2007).

In addition to transcriptional and post-translational regulation, there is growing evidence that epigenetic repression mediated by Polycomb group (PcG) proteins is an integral part of the Notch signaling regulatory network (Acharyya et al., 2010; Felician et al., 2014; Feng et al., 2011; Jin et al., 2017; Loubiere et al., 2016; Martinez et al., 2009; Schwanbeck, 2015). For Notch receptors, PcG protein recruitment has been detected at the *Notch* loci, highlighting the possibility that the Notch receptor dose may be additionally regulated at the epigenetic level. Specifically, members of Polycomb repressive complex 2 (PRC2) Su(Z)12 and EZH2 bind to the promoter region of the *Notch1* and *Notch3* loci in cultured mammalian cells, but the effect of the PRC2 recruitment on *Notch* expression has not been determined (Acharyya et al., 2010; Jin et al., 2017). In the *Drosophila* eye, *Notch* expression is elevated when the *polyhomeotic* (*ph-p* and *ph-d*) gene, which encodes a core component of the PRC1, is mutated. This is closely related to the observed deposition of Ph and Pc (another member of the PRC1) in the promoter region of the *Notch* locus (Loubiere et al., 2016; Martinez et al., 2009). However, PRC1 proteins are known to bind to loci other than *Notch*, including key members of the JNK, JAK-STAT and Wingless (Wg) signaling cascades (Classen et al., 2009; Loubiere et al., 2016). Given the extensive crosstalk between Notch and the developmental signaling pathways described above (Beira et al., 2018; Feng et al., 2011; Torres et al., 2018), it is uncertain whether the observed effect of PRC1 on *Notch* expression during fly eye development is direct.

[1]Ministry of Education Key Laboratory of Cell Proliferation and Differentiation, School of Life Sciences, Peking University, Beijing 100871, China. [2]Peking-Tsinghua Joint Center for Life Sciences, Academy for Advanced Interdisciplinary Studies, Peking University, Beijing 100871, China. [3]Department of Entomology, China Agricultural University, Beijing 100193, China.
*These authors contributed equally to this work

‡Authors for correspondence (liumin02@pku.edu.cn; zhua@pku.edu.cn)

A.J.Z., 0000-0002-3370-5125

Handling Editor: Haruhiko Koseki
Received 13 September 2022; Accepted 5 May 2023

Development (2023) 150, dev201297. doi:10.1242/dev.201297

Epigenetic phenomena were first reported in *Drosophila*, and experimentally validated epigenetic targets all contain cis-regulatory elements called Polycomb response elements (PREs) that recruit PcG proteins to their respective genomic loci (Grossniklaus and Paro, 2014; Kassis et al., 2017; Schuettengruber et al., 2017). As no functional PREs have been detected at the *Notch* locus, it is necessary to identify physiologically relevant PREs to establish a direct role of PcG in controlling the Notch receptor dose in *Drosophila*. In this study, we found that Stuxnet (Stx), an upstream epigenetic regulator that controls PRC1 stability and assembly (Du et al., 2016), positively regulates *Notch* mRNA expression, thus providing us with an excellent opportunity to evaluate the direct contribution of epigenetic regulation of the Notch receptor dose. We showed that Stx is a positive regulator of Notch signaling in multiple developmental processes. It epigenetically controls *Notch* receptor gene transcription by removing Pc from a previously uncharacterized PRE at the *Notch* receptor gene locus. Unlike those PcG-binding sites mapped to the *Notch* locus by chromatin immunoprecipitation sequencing (ChIP-seq) (Ahmad and Spens, 2019; Loubiere et al., 2016; Martinez et al., 2009), this new PRE, named *Notch* PRE, is responsive to altered Stx and PRC1 activities, providing *in vivo* evidence that *Notch* is a bona fide PcG target. Although PcG deposition has been found at many genomic loci through 'omics' studies, *in vivo* evidence supporting the physiological relevance of epigenetic regulation to specific targets is lacking, in part because, in most cases, epigenetic regulation can only fine-tune development, which is often counteracted by the intrinsic genetic and cellular plasticity of the embryo to ensure developmental robustness (De et al., 2016; Mihaly et al., 1997; Ogiyama et al., 2018; Sipos et al., 2007; Xiao et al., 2022). We show that the new *Notch* PRE identified in our study is functional *in vivo*. Deleting this PRE *in situ* from the *Notch* locus increases *Notch* mRNA expression, resulting in loss of macrochaetes in the notum and excessive crystal cell differentiation in the lymph gland: two stereotypical phenotypes associated with hyperactivation of Notch signaling. As cell fate specification in macrochaetes and in lymph gland development is highly sensitive to changes in Notch activity, *in situ* PRE deletion in such systems, which requires precise and robust control, may help to definitively determine the physiological role of epigenetic regulation in development.

RESULTS

stx positively regulates Notch signaling in *Drosophila*

To examine whether the upstream epigenetic regulator Stx regulates Notch signaling, we manipulated *stx* expression in the posterior compartment of the *Drosophila* wing (Fig. 1A-F″) and found that knockdown of *stx* by RNAi resulted in loss of marginal tissue in adult wing blades (compare Fig. 1C with 1A), resembling the stereotypical phenotype associated with reduced Notch signaling (Xu et al., 1990). To eliminate off-target effects of RNAi, we used two additional RNAi lines that target different regions in the *stx*-coding sequence (Fig. S1A). When overexpressed, both RNAi lines led to downregulated Notch signaling in adult wings (Fig. S1B-C′). Furthermore, the wing-notching phenotype observed in *stx* RNAi flies could be largely rescued by *stx* overexpression (Fig. S1D,E), using either a GS line that inserts the UAS element upstream of the *stx*-coding sequence (Toba et al., 1999) or a UAS-*stx* transgenic line (Du et al., 2016).

To confirm that Notch signaling is indeed regulated by *stx*, we examined the expression of Notch signaling targets *cut* and *wg*, as well as *NRE-gfp*, a Notch signaling reporter indicating that cells exhibit Su(H)-dependent activation of Notch signaling (Saj et al., 2010), in third instar larval wing imaginal discs. As expected, when *stx* expression was knocked down by RNAi in the posterior compartment of the wing disc, we observed decreased expression of Cut and Wg (Fig. 1D-D″), and reduced activity of the *NRE-gfp* reporter (Fig. S1G,G′). Furthermore, a similar wing-notching phenotype and reduced expression of Notch signaling target genes were observed when the YFP protein trap line CPTI-004181, with a *yfp* cassette inserted in frame at the *stx* locus and a reported trapping efficiency of 68% (Du et al., 2016), was used for destabilizing endogenous Stx-YFP fusion proteins using the anti-GFP nanobody (Fig. S1I-J′; Caussinus et al., 2012). In contrast to the effects associated with reduced *stx* activity, overexpression of *stx* resulted in loss of vein tissue (Fig. 1E), a phenotype associated with increased Notch signaling (Xu et al., 1990), and corresponding increases in Cut and Wg expression, and in *NRE-gfp* activity (Fig. 1F-F″; Fig. S1H,H′).

To further determine the involvement of *stx* in Notch signaling, we examined the genetic interactions between *stx* and various Notch pathway components. We found that the wing-notching phenotype caused by *stx* RNAi could be further enhanced by loss-of-function alleles of positive regulators of Notch signaling, such as $Notch^{1}$, $Notch^{PL24}$, Ser^{1} and mam^{8} (Fig. S1K-O). Consistently, this *stx* RNAi phenotype was suppressed by the loss-of-function allele of *Suppressor of deltex* [*Su(dx)*], a negative regulator of Notch signaling (Fig. S1P; Wilkin et al., 2004). These data suggest that *stx* plays a positive role in Notch signaling in wing development.

As the regulation and outcome of Notch signaling often depends on the cellular context (Bray, 2016), we investigated whether *stx* promotes Notch signaling in tissues other than the developing wing. The specification of *Drosophila* sensory organ precursors (SOPs) in the developing adult notum and crystal cells in the lymph gland is highly sensitive to fluctuating Notch signaling (Brennan et al., 1999; Jung et al., 2005; Kopan, 1999; Lan et al., 2020; Lebestky et al., 2003). Impaired Notch activity leads to supernumerary SOPs and reduced crystal cell specification, whereas overactivation of Notch signaling results in SOP loss and crystal cell overproduction. The adult scutellum contains four bristles derived from two SOPs, aSC and pSC, in the notum of the larval wing disc (Fig. 1G,H; Hartenstein and Posakony, 1989). We examined the requirement of *stx* in scutellar bristle development by manipulating *stx* expression using a *patched* (*ptc*)-Gal4 driver whose expressing domain in notum spans aSC and pSC (Fig. 1H; Brennan et al., 1999). Reduced *stx* expression by RNAi increased the number of scutellar bristles and the number of *neuralized* (*neur*)-lacZ-labeled SOPs (Fig. 1I,J,M; Huang et al., 1991). Conversely, increased *stx* activity prevented scutellar bristle development and SOP specification (Fig. 1K-M). We used *lozenge* (*lz*)-Gal4 to regulate *stx* expression in crystal cells and found that knocking down *stx* significantly reduced the number of crystal cells labeled by *lz*>GFP and Notch (Fig. 1O,O′,Q; Lebestky et al., 2000), whereas elevated *stx* expression enhanced crystal cell specification (Fig. 1P,Q). To rule out the possibility that the decrease in the number of crystal cells caused by *stx* knockdown is a consequence of induced apoptosis, we examined the protein levels of cleaved Dcp-1 caspase, an indicator of apoptosis, in the lymph glands and found that knocking down *stx* expression did not induce the cleavage of Dcp-1 (Fig. S1Q-Q″). Based on the above observations, we conclude that *stx* is a general positive regulator of Notch signaling in *Drosophila*.

Stx regulates *Notch* mRNA expression through its effects on PRC1

Our previous study showed that Stx promotes proteasomal degradation of the Pc protein, a core component of the epigenetic repressive PRC1

Development (2023) 150, dev201297. doi:10.1242/dev.201297

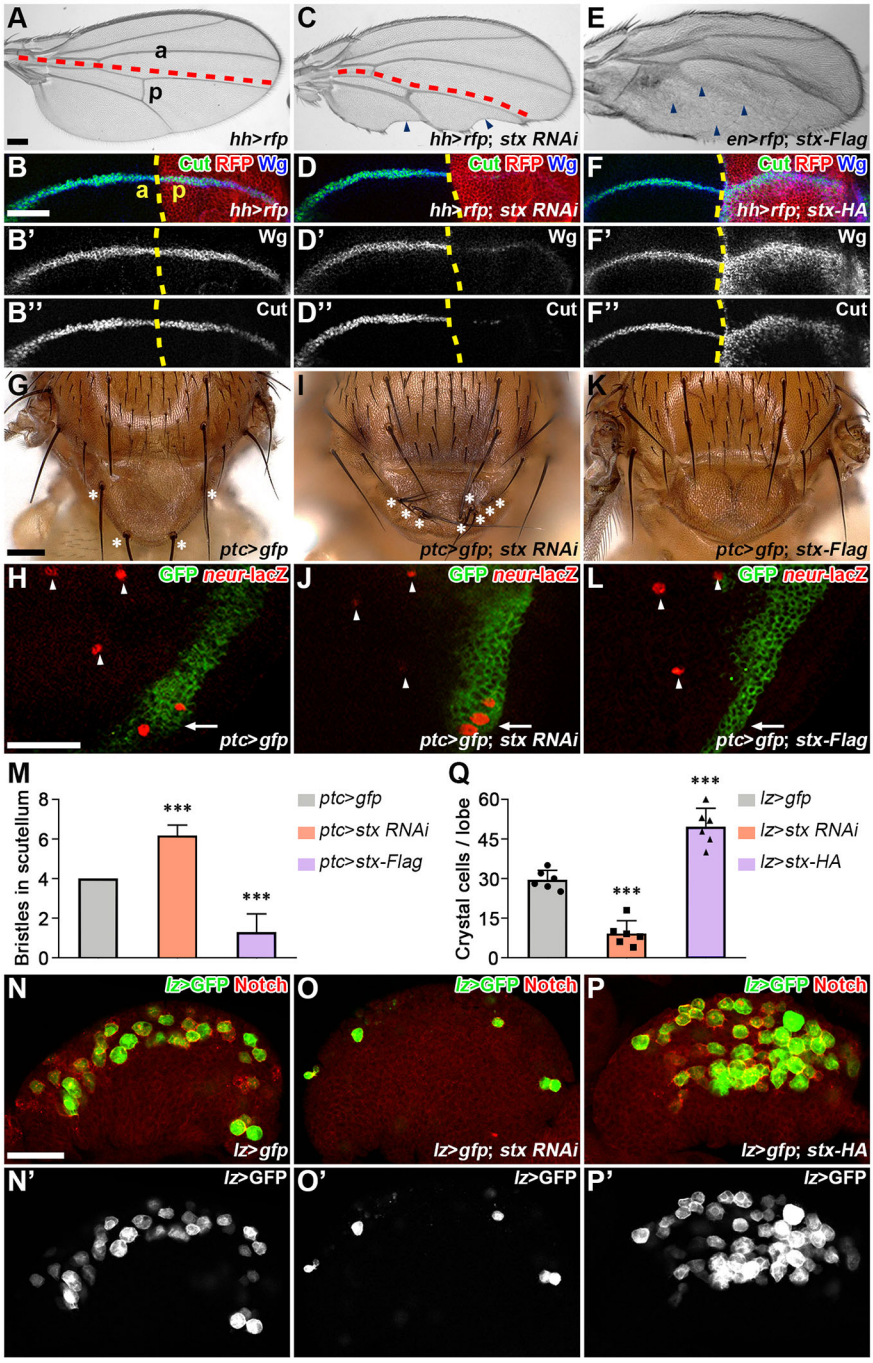

Fig. 1. *stx* is a positive regulator of Notch signaling in *Drosophila* development. (A-F″) Adult wings (A,C,E), Wg and Cut expression in wing discs (B-B″,D-D″,F-F″) of the indicated genotypes are shown. Knocking down *stx* in the posterior compartment using *hh*-Gal4 leads to stereotypical notched wing margin formation (arrowheads in C), whereas overexpression of *stx* in the posterior compartment using *en*-Gal4 results in loss of vein tissues (arrowheads in E). When *stx* expression is reduced by RNAi, the Notch signaling targets Wg (D′, compare with B′) and Cut (D″, compare with B″) are downregulated. Conversely, when *stx* is overexpressed, Wg (F′, compare with B′) and Cut (F″, compare with B″) expression increases. RFP marks the posterior compartment of the wing disc expressing *hh*-Gal4. Adult wings are shown with proximal to the left, with anterior/posterior (a/p) boundaries marked with red dashed lines. Wing discs are shown with anterior to the left and ventral at the top, with a/p boundaries marked with yellow dashed lines. (G-L) Adult nota (G,I,K) and *neur*-lacZ expression in wing discs (H,J,L) of the indicated genotypes. When *ptc*-Gal4-driven RNAi reduces *stx* expression, the number of scutellar bristles and *neur*-lacZ-labeled SOPs in the GFP-marked RNAi-expressing region increases (asterisks in I and arrow in J, compare with G and H). Conversely, overexpression of *stx-Flag* results in a decrease in the number of scutellar bristles and SOPs (K and arrow in L, compare with G and H). SOPs outside the GFP-expression region (arrowheads in H,J,L) are not affected by *stx* manipulation. (M) The mean number of bristles per scutellum of the indicated genotype (n=17). Error bars represent s.d. ***P<0.001 (one-way ANOVA, Dunnett's multiple comparison tests). (N-P′) *lz*>GFP and Notch expression in lymph glands of the indicated genotypes. When *stx* is knocked down by RNAi, the number of *lz*>GFP-labeled crystal cells decreases (O′, compare with N′). Conversely, when *stx* is overexpressed, *lz*>GFP-labeled crystal cells are overproduced (P′, compare with N′). (Q) The mean number of crystal cells per primary lobe in lymph glands of the indicated genotype (n=6). Error bars represent s.d. ***P<0.001 (one-way ANOVA, Dunnett's multiple comparison tests). Scale bars: 100 µm in A,C,E,G,I,K; 50 µm in B-B″,D-D″,F-F″, H,J,L,N-P′.

complex, thereby disrupting the assembly and activity of PRC1 (Du et al., 2016). In addition to Pc, *Drosophila* PRC1 is made up of three other proteins, including Ph, Posterior sex combs (Psc) and Sex combs extra (Sce). As increased expression of the *Notch* receptor and its ligand *Serrate* (*Ser*) but not the other ligand *Delta* (*Dl*) was observed in the *ph* and *Psc* mutant eye discs (Loubiere et al., 2016; Martinez et al., 2009), we investigated whether Stx positively regulates Notch signaling in the developing wing by regulating the expression of *Dl*, *Ser* or *Notch*. We found that when *stx* was knocked down in the wing disc, the expression levels of both Notch ligands, Dl and Ser, were not affected (Fig. S2A-D′). However, the expression pattern of *Dl* changed from two stripes adjacent to the D-V boundary to one stripe overlapping the D-V boundary (Fig. S2E-E″). This phenotype has been observed in wing discs carrying temperature-sensitive *Notch* (*Notch*^{ts}) mutations (de Celis and Bray, 1997), thus suggesting that Notch receptor expression may be affected. We consistently found a significant reduction in the amount of Notch protein in *stx* knockdown cells (Fig. 2B,B′, compare with 2A). Conversely, when *stx* was overexpressed, Notch expression increased significantly (Fig. 2C,C′; compare with 2A).

To further determine whether regulation of Notch by Stx occurs at the transcriptional or post-transcriptional level, we performed fluorescence *in situ* hybridization in the wing disc and found that *Notch* mRNA was greatly reduced when *stx* was knocked down (Fig. 2E, compare with 2D). Conversely, overexpression of *stx* resulted in elevated *Notch* expression (Fig. 2F, compare with 2D). Regulation of *Notch* receptor mRNA expression by *stx* was also quantified by quantitative real-time PCR (qPCR). When *stx* expression in the wing

Development (2023) 150, dev201297. doi:10.1242/dev.201297

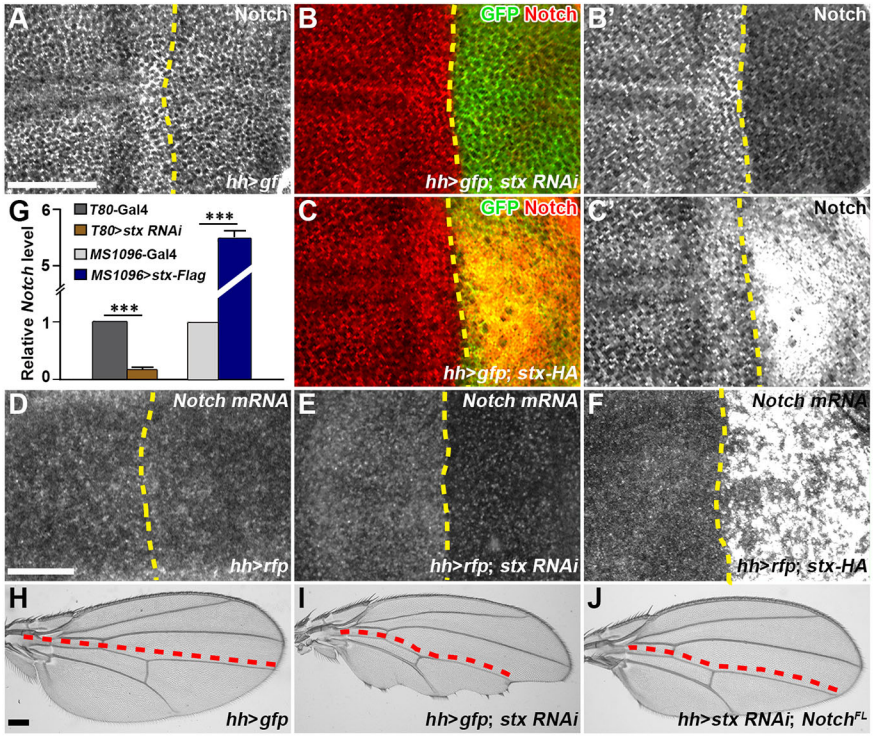

Fig. 2. Stx positively regulates *Notch* gene transcription. (A-C′) Notch expression in wing discs of the indicated genotype is shown. Notch protein is uniformly expressed in the anterior and posterior cells of the wing disc (A). Notch protein levels decrease when *stx* expression is reduced by *hh*-Gal4-driven RNAi (B′, compare with A). Conversely, when *stx* is overexpressed, Notch expression increases (C′, compare with A). GFP marks the *hh*-Gal4-expressing posterior compartment of the wing disc. (D-G) *Notch* mRNA detected in the wing disc of the indicated genotype by fluorescence *in situ* hybridization (D-F) and qPCR (G) is shown. *Notch* mRNA is uniformly expressed in the anterior and posterior compartments of the wing disc (D). When *stx* is knocked down by *hh*-Gal4-driven RNAi in posterior compartment cells, *Notch* mRNA decreases (E, compare with D). Conversely, *Notch* mRNA is elevated when *stx* is overexpressed using *hh*-Gal4 (F, compare with D). (G) *Notch* mRNA expression was quantified by qPCR after manipulating *stx* activity. The bar graph represents relative *Notch* mRNA levels of indicated genotype (n=3). Error bars represent s.d. ***P<0.001 (two-tailed Student's t-test). (H-J) Adult wings of the indicated genotype are shown. The wing notching phenotype induced by *stx RNAi* (I, compare with H) is largely rescued when $Notch^{FL}$ and *stx RNAi* are expressed simultaneously (J, compare with H and I). Adult wings are shown with proximal to the left, with a/p boundaries marked with red dashed lines. Wing discs are shown with anterior to the left and ventral at the top, with a/p boundaries marked with yellow dashed lines. Scale bars: 50 µm in A-F; 100 µm in H-J.

disc was knocked down by *T80*-Gal4, *Notch* mRNA levels were reduced by 80%, whereas increased *stx* activity produced by *MS1096*-Gal4 resulted in a fivefold upregulation of *Notch* mRNA expression (Fig. 2G). Furthermore, we showed that the wing-notching phenotype caused by *stx* knockdown was largely rescued by overexpression of $Notch^{FL}$ (Fig. 2H-J). Therefore, we conclude that Stx positively regulates Notch signaling by promoting *Notch* mRNA expression.

As Stx is known to promote Pc protein degradation (Du et al., 2016), we investigated the possibility of Stx regulating *Notch* mRNA expression through Pc. As expected, removing a single copy of the *Pc* was sufficient to rescue the adult wing margin defects caused by reduced *stx* expression (Fig. 3B, compare with 3A). Consistent with this observation, *Notch* expression and activation of the Notch signaling targets *cut* and *wg* were also largely restored (Fig. 3E-F′, compare with. 3C-D′). Conversely, Notch upregulation induced by *stx* overexpression was abolished when *Pc* was co-expressed (Fig. 3H-H″, compare with 3G-G″). These results suggest that *Pc* is epistatic to *stx* and that the regulation of *Notch* mRNA expression by Stx may depend on Pc activity. This inference is further supported by the cell-autonomous enhancement of Notch protein production observed in the loss-of-function Pc^{XT109} clones in the wing disc (Fig. 3I-I″).

Increased *Notch* expression is observed when the *ph* or *Psc* function of the *Drosophila* eye disc is impaired (Loubiere et al., 2016; Martinez et al., 2009). Therefore, we asked whether the regulation of *Notch* by Stx also depends on other components of the PRC1 complex. As expected, removal of one copy of *ph* or *Psc* largely rescued the *stx* RNAi-induced wing-notching phenotype (Fig. 3J,K, compare with 3A). In contrast, this phenotype was unaffected when 50% of *Enhancer of zeste* [*E(z)*],which encodes the enzymatic subunit of the PRC2 complex responsible for depositing the H3K27me3 mark, was removed (Fig. 3L, compare with 3A). This result is consistent with a previous study showing that H3K27me3 modification may be dispensable for epigenetic repression of *Notch* (Loubiere et al., 2016). Taken together, the above results demonstrate that Stx promotes *Notch* mRNA expression by reducing PRC1 activity.

The *Notch* receptor gene is a bona fide neo-PRC1 target *in vivo*

In *Drosophila*, canonical PcG target genes often contain PRE at their respective genomic loci, which is a specific cis-regulatory sequence required for PRC recruitment (Grossniklaus and Paro, 2014). To identify functional PREs at the *Notch* locus, we performed DNA adenine methyltransferase identification by sequencing (DamID-seq) in wing imaginal discs and analyzed these data together with the two previously published ChIP-seq datasets (Ahmad and Spens, 2019; Loubiere et al., 2016). Similar to

Development (2023) 150, dev201297. doi:10.1242/dev.201297

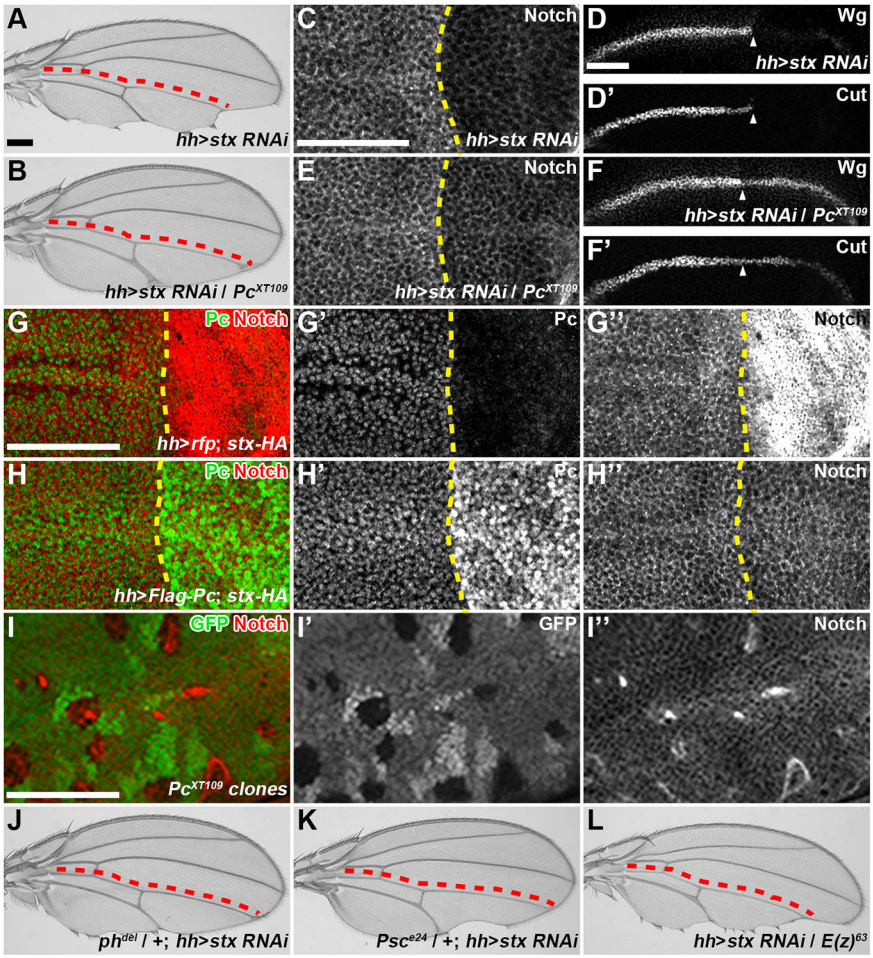

Fig. 3. Stx regulates Notch expression by reducing PRC1 activity. (A-F′) Adult wings (A,B) and protein production of Notch, Wg and Cut in wing discs (C-F′) of the indicated genotype are shown. Knocking down *stx* by *hh*-Gal4-driven RNAi results in a posterior wing-notching phenotype (A), and reduced Notch (C), Wg (D) and Cut levels (D′) in posterior wing disc cells. These phenotypes are largely restored by removing 50% of endogenous *Pc* using a loss-of-function Pc^{XT109} allele (B, compare with A and E-F′, compare with C-D′). The arrowhead marks the a/p boundary of the wing disc (D,D′,F,F′). (G-H″) Pc and Notch expression in wing discs of the indicated genotype are shown. Overexpression of *stx* by *hh*-Gal4 in posterior cells promotes Pc degradation (G′) and enhanced Notch expression (G″). When *Pc* (H′) and *stx* are co-expressed, the upregulation of Notch is eliminated (H″, compare with G″). (I-I″) Notch expression is elevated in Pc^{XT109} somatic clones (I″), which are negatively marked by GFP (I′). (J-L) Adult wings of the indicated genotype are shown. The posterior wing-notching phenotype caused by *stx* knockdown is substantially rescued by ph^{del}, an amorphic *ph* allele (J, compare with A) or Psc^{e24}, a loss-of-function *Psc* allele (K, compare with A), but not by $E(z)^{63}$ (L, compare with A), which is an amorphic *E(z)* allele. Adult wings are shown with proximal to the left, with a/p boundaries marked with red dashed lines. Wing discs are shown with anterior to the left and ventral at the top, with a/p boundaries marked with yellow dashed lines. Scale bars: 100 µm in A,B,J-L; 50 µm in C-I″.

the two published ChIP-seq datasets, DamID-seq showed significant Pc recruitment to canonical PcG target genes, including *Ultrabithorax* (*Ubx*), *bithoraxoid* (*bxd*), *abdominal A* (*abd-A*), *iab-8* and *Abdominal B* (*Abd-B*). Consistent with the role of Stx in reducing Pc activity, Pc recruitment was lost at these loci when *stx* was overexpressed (Fig. S3A; Du et al., 2016). However, Pc recruitment to the *Notch* locus revealed by the DamID-seq data in this study did not fully conform to what was found in a previously published ChIP-seq data (Ahmad and Spens, 2019; Loubiere et al., 2016; Fig. S3B). Therefore, we treated all Pc-bound regions in the *Notch* locus revealed by three different datasets as putative PREs, which we named *E1-E7* (Fig. 4A; Fig. S3B). Among them, *E1* was identified by all three datasets, while *E4* and *E6* were identified by ChIP-seq data from Ahmad and Spens (2019) and by DamID-seq data from this study. Furthermore, *E2* and *E7* were only identified by ChIP-seq data from Ahmad and Spens (2019), while *E3* and *E5* were identified only by DamID-seq data from this study (Fig. S3B). Similar to the canonical PcG targets, the binding of Pc to *E1*, *E3*, *E4*, *E5* and *E6* was greatly reduced when *stx* was overexpressed (Fig. S3B), further supporting the observation that Stx promotes *Notch* receptor mRNA expression by preventing PRC1 recruitment to the *Notch* locus.

To determine whether these Pc-binding regions are functional PREs *in vivo*, we constructed a set of PRE-GFP reporter plasmids in which nuclear GFP expression is jointly controlled by a quadrant enhancer of the *vestigial* gene (vg^{QE}) and one of seven putative PREs flanked by two FRT sites (Sengupta et al., 2004). The presence of functional PRE is expected to repress vg^{QE}-mediated GFP expression, whereas excision of the PRE should restore GFP expression (Fig. 4B). These plasmids were integrated into the same *attP2* landing site in the *Drosophila* genome by ϕC31 integrase, generating seven transgenic fly lines for *in vivo* analysis of putative PRE function. We found that GFP expression regulated by *E1* or *E5*, but not by *E2*, *E3*, *E4*, *E6* or *E7*, showed a significant reduction in wing imaginal discs compared with vg^{QE} alone (Fig. 4C-E,L; Fig. S4B-I′,L). Notably, *E5* inhibited vg^{QE}-mediated GFP expression more strongly than *E1* (Fig. 4D,E,L, compare with 4C′; Fig. S4C′,G′,L compare with S4B′). When *E1* or *E5* was excised by *en*-Gal4-driven flippase expression in the posterior compartment of the wing disc, vg^{QE}-GFP expression was restored (Fig. 4F-G′,M), implying that *E1* and *E5* are responsible for the decrease in GFP expression. However, when *Pc* was knocked down or *stx* was overexpressed in the posterior compartment of the wing disc, only the inhibitory effect of *E5* was attenuated, whereas *E1* was not (Fig. 4H-K′,M), suggesting that only the function of *E5* depends on endogenous PcG activity, and *E1* cooperates with factors other than PcG proteins to repress *Notch* expression. This conclusion is further supported by the observation that loss of *ph* (Fig. S4J,J′,M compare with Fig. S4G′) or knockdown of *Psc* (Fig. S4K,K′,N, compare with S4G′) significantly increased GFP expression of the *E5* reporter. *E5* spans the ∼1 kb region (ChrX: 3,153,915-3,155,043; r6.49) located in the second intron of the *Notch* locus (Fig. S3B). It does not overlap with any known *Notch* regulatory sequence, but contains 32 putative binding sites for Pho, GAF, or DSP1 (Fig. S3C), all of

Development (2023) 150, dev201297. doi:10.1242/dev.201297

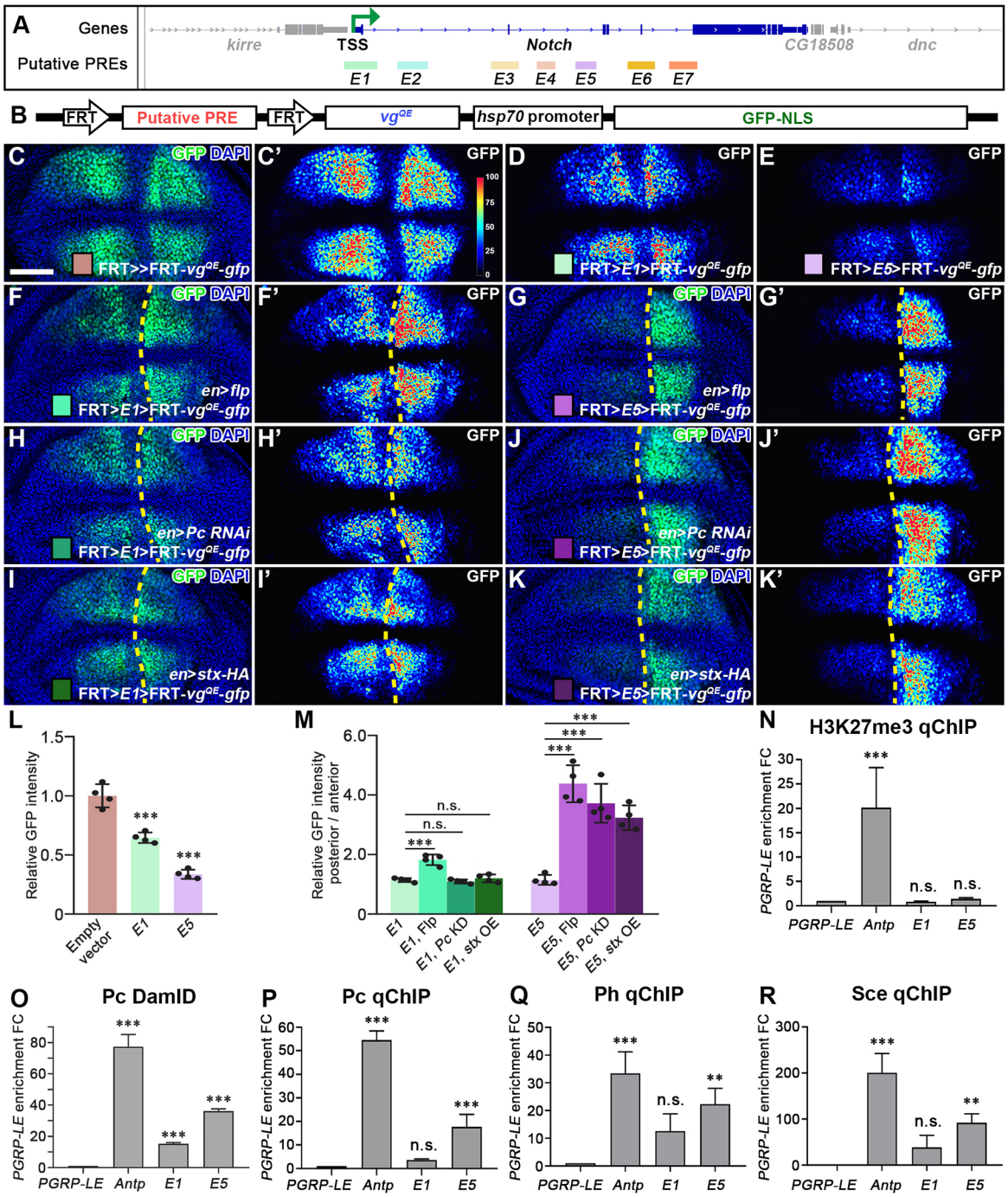

Fig. 4. Identification of the functional PRE at the *Notch* locus. (A) Schematic diagram of the putative PREs (rectangles) in the *Notch* locus where each putative PRE is assigned a unique color key that matches the PRE GFP reporter activity shown in L and M. (B) Schematic diagram of the PRE reporter. GFP reporter expression is jointly controlled by the vg^{QE} enhancer and putative PRE. (C-K′) GFP reporter expression (C,F-K) and corresponding heatmap images (C′,D,E,F′-K′) in wing discs of the indicated genotype are shown. The vertical color bar on the right (C′) represents the intensity range. Compared with GFP reporter activity controlled by only vg^{QE} (C′), adding *E1* to the reporter construct slightly represses GFP reporter expression (D, compare with C′), while *E5* strongly inhibits GFP expression (E, compare with C′). GFP reporter expression is restored upon removal of *E1* (F′) or *E5* (G′) by the flippase-mediated flip-out strategy in the posterior compartment of the wing disc (indicated by square brackets). Reducing PcG activity by overexpressing *stx* or knocking down *Pc* has little effect on *E1*-GFP reporter expression (H′,I′), but significantly increases *E5*-GFP expression (J′,K′). (L,M) Statistical analyses of relative GFP fluorescence intensity in wing discs of the indicated genotype (n=4). GFP activity controlled only by vg^{QE} is used as a normalized standard. Data are mean9±s.d. ***P<0.001, n.s. P>0.05 (one-way ANOVA, Dunnett's multiple comparison tests). (N-R) qChIP experiments with H3K27me3, Pc, Ph or Sce were performed using nuclear extracts from wild-type w^{1118} wing discs (N) and wing discs expressing *Pc-GFP* (P), *ph-GFP* (Q) or *Sce-Flag* (R). (O) DamID-qPCR was performed in wing discs expressing *Dam* or *Pc-Dam* to compare Pc recruitment in *E1* and *E5* regions. H3K27me3 status and Pc, Ph and Psc recruitment at regions *E1* and *E5* of the *Notch* locus are shown. *PGRP-LE* was used as a negative control for normalization. *Antp*, a widely studied PcG target gene, was used as a positive control. Experiments were performed in triplicate and data are mean±s.d. ***P<0.001, **P<0.01, n.s. P>0.05 (one-way ANOVA, Dunnett's multiple comparison tests). Wing discs are shown with anterior to the left and ventral at the top, with a/p boundaries marked with yellow dashed lines. Scale bar: 50 µm.

Development (2023) 150, dev201297. doi:10.1242/dev.201297

which are transcription factors reported to be involved in PcG recruitment (Déjardin et al., 2005; Grossniklaus and Paro, 2014; Schuettengruber et al., 2017). We believe that a detailed analysis of the binding of these transcription factors to *E5* will provide mechanistic insights into epigentic control of *Notch* receptor gene transcription.

Notch has previously been classified as a neo-PRC1 target because only PRC1 recruitment, but no H3K27me3 modification marks, was detected around the *Notch* locus (Loubiere et al., 2016). Therefore, we performed quantitative chromatin immunoprecipitation (qChIP) and DamID-qPCR in the wing imaginal disc to examine whether *E5* is sufficient to recruit PRC1 in the absence of H3K27me3 modification. As shown by the qChIP and DamID-qPCR assays, significant recruitment of Pc, Ph and Sce was detected at *E5*, but without the H3K27me3 modification mark (Fig. 4N-R). Moreover, these PRC1 components bound *E5* more strongly than *E1* (Fig. 4O-R), echoing the conclusion that *E5* may be more important than *E1* in PRC1 recruitment. Combined with the above PRE reporter analysis, we identified *E5* as a functional PRE at the *Notch* locus, regulated by PcG. Therefore, we name *E5* as the '*Notch* PRE'. In conclusion, we provide evidence that *Notch* is a bona fide neo-PRC1 target and that epigenetic regulation of Notch dose is mainly mediated through our newly discovered *Notch* PRE. Given that *Notch* PRE is the first experimentally verified PRE of neo-PRC1 targets, this PRE will serve as a starting point for understanding the mechanisms underlying the dynamic regulation of *Notch*, as well as the growing class of PRC1 target genes (Loubiere et al., 2016) that acquire little or no H3K27me3, resulting in transient silencing.

The *Notch* PRE is indispensable for Notch receptor dose control *in vivo*

To investigate the physiological role of this *Notch* PRE, we generated a $Notch^{\Delta PRE}$ mutant allele in which the *Notch* PRE was removed *in situ* from the *Notch* locus by CRISPR-Cas9-mediated homologous recombination (Fig. S5A). The removal of *Notch* PRE, confirmed by PCR and Sanger sequencing (Fig. S5B,C), resulted in an ∼30% increase in *Notch* mRNA expression in $Notch^{\Delta PRE}$ mutant larvae (Fig. 5A,B). Based on the above PRE reporter analysis and genetic interactions, we believe that after removing the PRE *in situ* from the *Notch* locus, *Notch* expression is no longer regulated by Stx. Consistent with this speculation, the notched adult wing phenotype and downregulation of Notch, Wg and Cut expression caused by *stx* RNAi were largely restored in the context of $Notch^{\Delta PRE}$ mutation (Fig. S5G-I′, compare with S5D-F′). Genetic interactions further support this view, as the adult wing morphology of $Notch^{\Delta PRE}$ could not be altered against the background of Pc^{3} heterozygotes (Fig. S5L, compare with S5K,J). Of note, the posterior wing margin curvature phenotype shown by the Pc^{3} heterozygotic mutation (Fig. S5K,L) is a homeotic transformation phenotype unrelated to *Notch* hyperactivation (Bi et al., 2022).

Given the importance of Notch receptor dose in Notch signaling homeostasis, the loss of *Notch* PRE-mediated PRC1 repression may impair developmental processes that are sensitive to changes in Notch activity. As expected, we found that $Notch^{\Delta PRE}$ flies exhibited loss of notal and scutellar macrochaetae, and excessive crystal cell differentiation in the lymph gland, two stereotypical phenotypes associated with hyperactivation of Notch signaling (Brennan et al., 1999; Jung et al., 2005; Kopan, 1999; Lan et al., 2020; Lebestky et al., 2003). The number of dorsocentral bristles (DCs) and scutellar bristles (SCs) in adult $Notch^{\Delta PRE}$ flies was significantly decreased (Fig. 5D,E, compare with 5C), which was consistent with the decrease in the number of *neur*-lacZ-labeled SOPs in the wing imaginal disc of $Notch^{\Delta PRE}$ larvae (Fig. 5G, compare with 5F). Furthermore, Lz-GFP (*piggyBac* insertion allele of *lz*) and Notch antibody labeled crystal cells increased by approximately 50% in the primary lobes of the lymph glands of the third instar $Notch^{\Delta PRE}$ larvae (Fig. 5I-J, compare with 5H′). These results highlight the crucial role of *Notch* PRE in cell fate decisions that are highly sensitive to changes in Notch activity.

Although the loss of *Notch* PRE did not result in apparent defects in the developing wings, probably due to the need for further refinement and correction of the wing patterning process during the pupal stage, the genetic interactions between $Notch^{\Delta PRE}$ and classical *Notch* alleles still support the role of this PRE in Notch receptor dose control in wing development. Specifically, one copy of $Notch^{\Delta PRE}$ completely rescued the phenotypes caused by loss-of-function $Notch^{55e11}$/+, including overproduction of scutellar bristles and notched wings (Fig. 5K-N; de Celis et al., 1993, 1991). Furthermore, in trans-heterozygotes of $Notch^{\Delta PRE}$ and $Notch^{Ax\text{-}E2}$, a gain-of-function allele that does not show any defects in scutellar bristle development under heterozygosity (Fig. 5T; Xu et al., 1990), scutellar bristles were more extensively lost than in heterozygous $Notch^{\Delta PRE}$ alone (Fig. 5U,V, compare with 5S). Taken together, the above results suggest that *Notch* PRE is an integral part of the Notch receptor dose-controlling developmental process in the Notch signaling network.

DISCUSSION

Taking advantage of the power of *Drosophila* genetics, we identified Stx as a new epigenetic regulator that positively controls Notch receptor dose. This mode of regulation is mainly mediated by a bona fide PRE in the *Notch* locus, repressing *Notch* mRNA expression independently of H3K27 trimethylation. Importantly, this PRE plays a physiologically crucial role in Notch receptor dose control in multiple developmental contexts.

PRE is an important cis-regulatory element for PcG-mediated epigenetic repression (Grossniklaus and Paro, 2014; Steffen and Ringrose, 2014). It was originally discovered in *Drosophila* as DNA sequences that recruit PcG proteins and maintain transcriptional silencing of reporter genes (Chan et al., 1994; Kassis, 1994; Simon et al., 1993). To date, extensive genome-wide ChIP-seq data have revealed clustered PcG protein-binding sites in the *Drosophila* genome, of which only a few have been confirmed as functional PREs by reporter gene analysis (Bauer et al., 2016). This partly explains why most PcG-binding genes are not derepressed when the PcG complex is dysfunctional (Cohen et al., 2018; Gargiulo et al., 2013; Loubiere et al., 2016; Morey et al., 2015; Pherson et al., 2017). In cultured *Drosophila* BG3 cells with reduced *ph* expression, only about 5% of the genes occupied by PcG proteins are significantly upregulated (Pherson et al., 2017), whereas in the eye discs of PcG mutants, this number does not exceed 30% (Loubiere et al., 2016). A similar phenomenon was observed in mice. When *Bmi1*, *Ring1a* or *Ring1b* (*Rnf2*) expression is reduced, only about 4.8-15% of PcG target genes are derepressed (Cohen et al., 2018; Gargiulo et al., 2013; Morey et al., 2015). These results confirm why many cis-regulatory elements that recruit PcG proteins have little effect in *in vivo* reporter assays (Cuddapah et al., 2012; Cunningham et al., 2010). By integrating our DamID-seq and published ChIP-seq data (Ahmad and Spens, 2019; Loubiere et al., 2016), we identified seven PRC1-binding regions at the *Notch* locus with varying degrees of binding strength. Our study suggests that binding strength is not necessarily a good predicator of the physiological requirement for these binding regions. Only in combination with *in vivo* reporter assays did we identify two

Development (2023) 150, dev201297. doi:10.1242/dev.201297

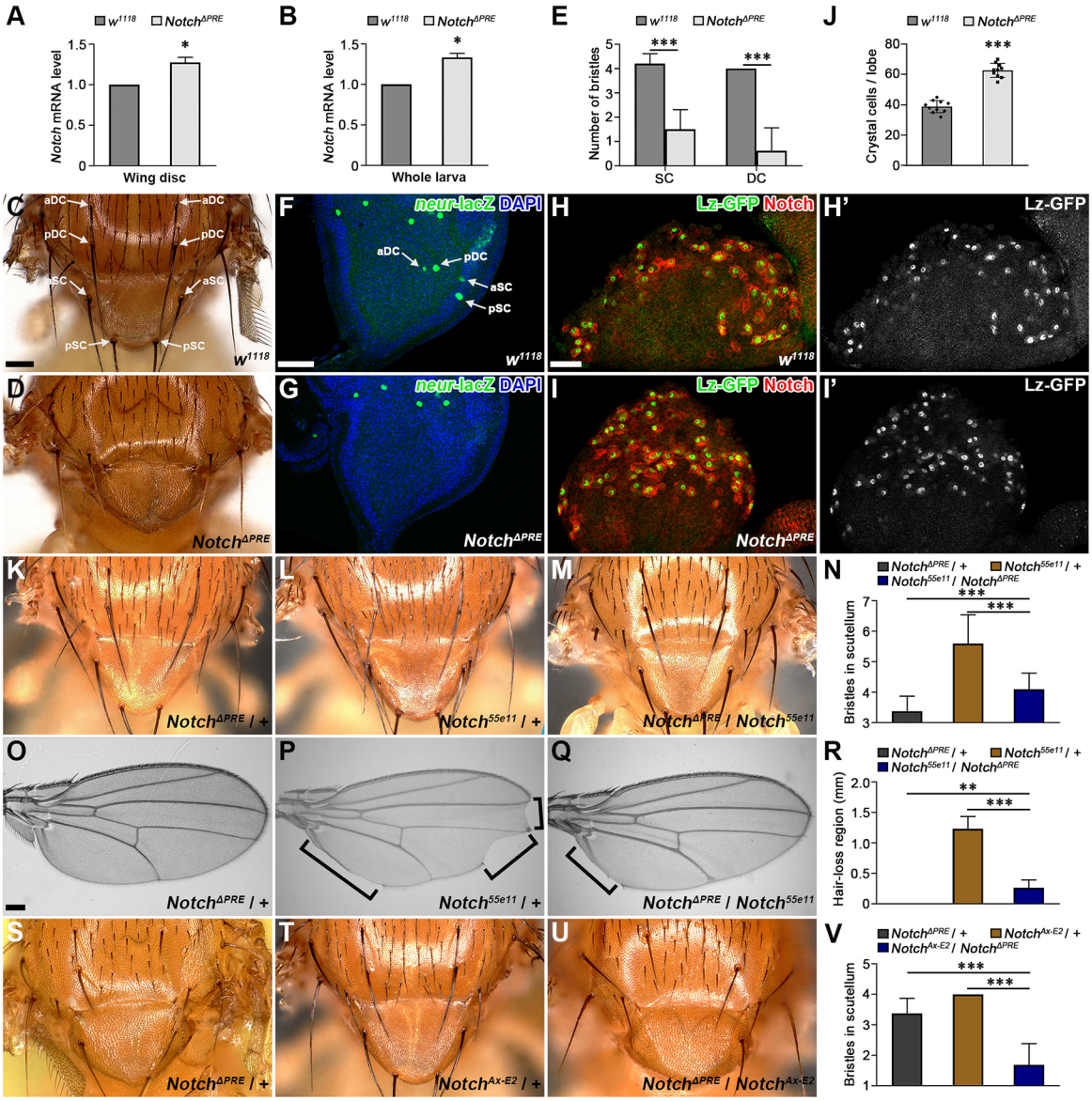

Fig. 5. *In situ* deletion of *Notch* PRE results in hyperactivation of Notch signaling during development. (A,B) *Notch* mRNA expression in the wing disc (A) and whole larvae (B) of w^{1118} and $Notch^{\Delta PRE}$ was quantified by qPCR. Bar graphs represent relative *Notch* mRNA levels of the indicated genotype (n=3); error bars represent s.d. *P<0.05 (two-tailed Student's t-test). (C-G) Adult nota (C,D) and *neur*-lacZ expression in wing discs (F,G) of the indicated genotype are shown. $Notch^{\Delta PRE}$ flies are defective in the development of notal and scutellar macrochaetae (D, compare with C). The number of DCs and SCs is significantly reduced (E). Consistently, *neur*-lacZ-labeled SOPs in wing discs that are determined to become DCs and SCs disappear (G; compare with F). (E) The mean number of DCs or SCs in adult nota of the indicated genotype (n=100). Error bars represent s.d. ***P<0.001 (two-tailed Student's t-test). (H-J) Expression of Lz-GFP and Notch in lymph glands of w^{1118} and $Notch^{\Delta PRE}$ is shown. The number of Lz-GFP-labeled crystal cells was significantly increased in $Notch^{\Delta PRE}$ larvae (I′; compare with H′). (J) The mean number of Lz-GFP positive cells per primary lobe of w^{1118} and $Notch^{\Delta PRE}$ larvae (n=10). Error bars represent s.d. ***P<0.001 (two-tailed Student's t-test). (K-R) The genetic interaction between $Notch^{\Delta PRE}$ and $Notch^{55e11}$, a loss-of-function allele of *Notch*. Adult nota (K-M) and wings (O-Q) of the indicated genotype are shown. (N,R) The mean number of bristles in the scutellum (N) and in the hair-loss region in wing margin (R) of the indicated genotypes (n=30). Error bars represent s.d. ***P<0.001, **P<0.01 (one-way ANOVA, Dunnett's multiple comparison tests). (S-V) The genetic interaction between $Notch^{\Delta PRE}$ and $Notch^{Ax\text{-}E2}$, a hypermorphic allele of *Notch*. Adult nota of the indicated genotypes are shown (S-U). (V) The mean number of bristles in scutellum of the indicated genotypes (n=30). Error bars represent s.d. ***P<0.001 (one-way ANOVA, Dunnett's multiple comparison tests). Adult wings are shown with proximal to the left. Wing discs are shown with anterior to the left and ventral at the top. Scale bars: 100 µm in C,D,K-M,O-Q,S-U; 50 µm in F,G-I′.

PRC1-binding regions sufficient to mediate *Notch* gene repression, only one of which is shown to respond to epigenetic regulation by Pc and Stx *in vivo*. Notably, this experimentally validated PRE does not belong to the PRC1-binding sites with the highest binding strength identified in previously published ChIP-seq datasets. Therefore, our study demonstrates that, in PRE prediction, it is not only necessary to determine the binding of PcG proteins to genomic loci but also, more importantly, to directly test the role of PcG-binding sites by reporter assays, as well as *in situ* deletion of these PcG-binding sites in the corresponding genomic loci. This conclusion echoes concerns that high-throughput sequencing analysis alone only increases the number of associations and should be further validated to reveal causality in biological processes (Stern, 2022).

Development (2023) 150, dev201297. doi:10.1242/dev.201297

Although PRE is considered crucial for epigenetic silencing of target genes, there is little in-depth study of their physiological function. To date, only a few PREs in the *Drosophila* genome have been deleted to directly test their *in vivo* requirement, and the phenotypic consequences of PRE deletion vary. In one case, deletion of *Ubx* PRE leads to ectopic *Ubx* expression and homeotic transformation (Sipos et al., 2007), supporting the crucial role of PRE in mediating epigenetic repression. This contrasts with the effect of removing a characterized PRE of *iab-7*, which does not result in a visible phenotype (Mihaly et al., 1997). This may be due to the presence of other cis-regulatory PRE-like elements required for epigenetic gene repression. Alternatively, in the absence of a canonical PRE, compensatory mechanisms for developmental robustness can be activated, as in the case of epigenetic control of the *invected-engrailed* (*inv-en*) gene complex. After *in situ* removal of *inv-en* PRE, the remaining weak PcG-binding interactions between PcG domains can maintain epigenetically silenced 3D chromatin structures (De et al., 2016). A similar result was observed in PRE deletion of the *vg* gene (Ahmad and Spens, 2019). The exact mechanisms behind these paradoxical phenomena require further investigation.

Metazoans use a variety of genetic, epigenetic and cellular mechanisms to ensure developmental robustness to buffer against genetic perturbations or environmental fluctuations (Félix and Wagner, 2008; Spatz et al., 2021). In our study, the increased expression of *Notch* caused by PRE deletion alters transient and rapid decision-dependent cell fate specification in the notum and lymph gland, but does not result in significant defects in wing margin formation, a gradual developmental process that requires further refinement and correction in later developmental stages. These seemingly contradictory consequences of PRE deletion in different tissues may reflect the different plasticity of the developmental process conferred by genetic and cellular compensation, thereby adapting to changes in developmentally regulatory gene expression and heterogeneous cellular responses (Xiao et al., 2022). Although our *Notch* PRE deletion mutation does not readily exhibit the classical gain-of-function *Confluens* phenotype in the developing wing, it is sufficient to compensate for the loss-of-function wing-notching phenotype in the sensitized background. Similarly, *in vivo* deletion of PRE in the *dachshund* (*dac*) gene results in only a very mild tarsal transformation of the first leg, a phenotype that can be further enhanced when flies are reared at higher temperatures (Ogiyama et al., 2018). Consistent with these observations, ectopic *Notch* or *dac* activity is known to lead to broader defects (Anderson et al., 2006; Baonza and Freeman, 2005; Córdoba and Estella, 2014; Dong et al., 2001; Ku and Sun, 2017; Shen and Mardon, 1997), as opposed to the more limited phenotypes observed when the corresponding PRE is deleted *in situ*. Thus, context-dependent sensitivity to PRE-mediated epigenetic control highlights the integral role of epigenetic adaptation to genetic and environmental fluctuations during development.

MATERIALS AND METHODS

Fly genetics

All fly crosses were maintained at 25°C, except those listed in Table S1. The following fly stocks were obtained from the Bloomington *Drosophila* Stock Center: *ap* (*apterous*)-Gal4 (#3041), *ap*-lacZ (#5374), *dpp* (*decapentaplegic*)-Gal4 (#1553), *en* (*engrailed*)-Gal4 (#30564), *hh* (*hedgehog*)-Gal4, *nub*-Gal4 (#25754), Lz-GFP (#43954), mam^{8} (#1596), *MS1096*-Gal4 (#8860), $Notch^{1}$ (#6873), $Notch^{55e11}$ (#28813), *neur*-lacZ (#4369), *NRE-gfp* (#30727), *pPc*-Pc-GFP (#9593), Pc^{3} (#1730), ph^{410} (#5813), Psc^{e24} (#24155), *ptc*-Gal4 (#2017), *rotund* (*rn*)-Gal4 (#7405), Ser^{1} (#89), *spalt major* (*salm*)-Gal4 (#5818), $Su(dx)^{2}$ (#293), *T80*-Gal4 (#1878), UAS-*flp* (#4539), UAS-$Notch^{FL}$ (#26820), UAS-*Nslmb-vhhgfp4* (#38422), UAS-*Pc RNAi* (#33622) and w^{1118} (#3605). Three UAS-*stx RNAi* lines (GD27036, GD23946 and KK109495) and a UAS-*Psc RNAi* line (GD30587) were obtained from the Vienna *Drosophila* RNAi Center (VDRC). The *stx-yfp* protein trap line CPTI-004181 and the GS line for *stx* (GS200070) were obtained from the *Drosophila* Genetic Resource Center (DGRC). UAS-*stx-Flag* and UAS-*Flag-Pc* have been described previously (Du et al., 2016).

$E(z)^{63}$ was a gift from Peter Harte (Case Western Reserve University, Cleveland, OH, USA). *hs-flp*;; *ubi-gfp*, *FRT2A* was a gift from Jocelyn McDonald (Kansas State University, Manhattan, KS, USA). *lz*-Gal4, UAS-*gfp* (BL#6313) was a gift from Ying Su (Ocean University of China, Qingdao, China). $Notch^{Ax\text{-}E2}$ was a gift from Michelle Longworth (Cleveland Clinic, OH, USA). $Notch^{PL24}$ was a gift from Alain Vincent (Université Toulouse III, France) (Bourbon et al., 2002). Pc^{XT109} was a gift from Jürg Müller (Max-Planck Institute of Biochemistry, Munich, Germany) (Müller et al., 1995). ph^{del} was a gift from Jian Wang (University of Maryland, College Park, USA) (Feng et al., 2011). UAS-*Dam* was a gift from Andrea Brand (University of Cambridge, UK) (Southall et al., 2014). UAS-*pPc-ph-GFP* was a gift from Donna Arndt-Jovin (Max-Planck Institute for Biophysical Chemistry, Göttingen, Germany) (Ficz et al., 2005). UAS-*Sce-Flag* was a gift from Judith Kassis (National Institutes of Health, USA) (Langlais et al., 2012).

Transgenic flies expressing UAS-*Pc-Dam* were generated by *P*-element mediated germline transformation. UAS-*stx-HA* and GFP reporters for putative Notch PREs were integrated into *attP2* site using ϕC31 integrase-mediated recombination to generate transgenic flies. $Notch^{\Delta PRE}$ mutant was generated by CRISPR/Cas9-mediated homologous recombination (Port et al., 2014). Details of related plasmids and primers are provided in Table S2.

Immunofluorescence staining, *in situ* hybridization and imaging of adult fly structures

Standard procedures were used for wing disc immunofluorescence staining and *in situ* hybridization (Su et al., 2011). Lymph glands were immunofluorescently stained using the described protocol (Evans et al., 2014). The following primary antibodies were used for immunofluorescence staining: rabbit anti-β-galactosidase (1:4000; 55976; Cappel), mouse anti-β-galactosidase [1:200; 40-1A; Developmental Studies Hybridoma Bank (DSHB)], mouse anti-Cut (1:100; 2B10; DSHB), rabbit anti-cleaved Dcp-1 (1:400; 9578; Cell Signaling Technology), mouse anti-Dl (1:200; C594.9B; DSHB), rabbit anti-GFP (1:4000; A11122; Invitrogen), mouse anti-N^{icd} (1:200; C17.9C6; DSHB), rabbit anti-Pc (1:500; this study), rat anti-Ser (1:2000; a gift from Kenneth Irvine, Rutgers University, NJ, USA; Papayannopoulos et al., 1998), mouse anti-Wg (1:100; 2A1; DSHB) and rabbit anti-Wg (1:1000; this study). Primers used for RNA probes synthesis are listed in Table S2.

Fluorescence images were acquired with a Leica SP8 confocal microscope or a Zeiss Axio Imager Z1 microscope equipped with an ApoTome. Heatmap images were generated in ImageJ using the heatmap plugin. Figures were assembled in Adobe Photoshop CC. Minor image adjustments (brightness and/or contrast) were made in Adobe Photoshop CC.

Adult wings and nota were dissected and mounted as described previously (Zhu et al., 2003). The images of these adult tissues were acquired with a Leica DMIL inverted microscope (wings) or a Keyence VHX-7000 digital microscope (nota).

Antibody generation

Rabbit polyclonal antibodies were raised against amino acids 191-354 of the Pc protein (Schuettengruber et al., 2009) and amino acids 3-468 of the Wg protein (Brook and Cohen, 1996) (Abclonal Biotech), and affinity purified for immunofluorescence staining. The specificity of rabbit anti-Pc antibody was validated by *Pc* RNAi in the wing disc (Fig. S6A'). Staining pattern of rabbit anti-Wg antibody in the wing pouch (Fig. S6B) is similar to that of mouse anti-Wg antibody (4D4; DSHB) (Fig. S6C).

RNA isolation and quantitative real-time PCR

Total RNA of third instar larval wing discs was extracted using Eastep Super Total RNA Extraction Kit (LS1040; Promega). Reverse transcription was

performed with Eastep RT Master Mix Kit (LS2050; Promega). cDNA levels were quantified by real-time PCR in a 7500 real time PCR system (Applied Biosystems) using PowerUp SYBR Green Master Mix (A25741; Thermo Fisher Scientific). Relative fold changes of *Notch* mRNA levels were calculated using comparative CT method. Samples from three independent experiments were prepared and run in triplicate. Primers used for qPCR are listed in Table S2.

Quantitative chromatin immunoprecipitation

qChIP analyses of the wing disc were performed using the previously described protocol (Loubiere et al., 2017). For each qChIP experiments, ∼900 pairs of wing discs were collected and three biological replicates were performed. w^{1118} was used for H3K27me3 qChIP experiments. *pPc*-Pc-GFP transgenic flies, in which GFP-tagged Pc is expressed under the control of an endogenous *Pc* promoter (Dietzel et al., 1999), were used for qChIP experiments on Pc. For qChIP experiments with Ph or Sce, wing discs expressing UAS-*pPc-ph-GFP* (Ficz et al., 2005) or UAS-*Sce-Flag* (Langlais et al., 2012) under *nub*-Gal4 control were used. Rabbit anti-GFP (6 µg per IP; A11122; Invitrogen) for Pc-GFP and Ph-GFP, rabbit anti-H3K27me3 (3 µg per IP; ABE44-S; Millipore) and mouse anti-Flag (5 µg per IP; AT0022; Engibody) for Sce-Flag were used. Primers used for qPCR are listed in Table S2. The results were normalized using the *PGRP-LE* gene, which served as a negative control.

DNA adenine methyltransferase identification

The *Pc* cDNA was cloned into the pUAST-*attB-LT3-Dam* vector (a gift from Andrea Brand) (Southall et al., 2014), and transgenic flies were generated by integrating the vector at the *attP2* site. UAS-*Dam* transgenic flies were used as negative controls for nonspecific Dam activity. The genotypes used for the experiments were: *nub*-Gal4/+; UAS-*Dam*/+, *nub*-Gal4/+; UAS-*Dam-Pc*/+ and *nub*-Gal4/+; UAS-*Dam-Pc*/UAS-*stx-HA*. Crosses were raised at 25°C. For DamID-qPCR, 100 pairs of wing discs from each of three independent experiments were dissected from third instar larvae in ice-cold Schneider's *Drosophila* medium. For DamID-seq, 300 pairs of wing discs were dissected. The DamID was performed according to a previously described protocol (Vogel et al., 2007). The PCR products were purified by QIAquick PCR purification kit (Qiagen).

For DamID-qPCR, purified PCR products were used for real-time quantitative PCR analyses. Primers for qPCR are listed in Table S2. For DamID-seq, purified PCR products were used to generate the next-generation sequencing (NGS) libraries that were further sequenced via HiSeq 2500 and multiplexed to yield ∼50 million mapped reads per sample (Novogene). Using the damidseq_pipeline (http://owenjm.github.io/damidseq_pipeline/) (Marshall and Brand, 2015), NGS reads were aligned to the *Drosophila melanogaster* reference genome version r6.41 by bowtie2 (Langmead and Salzberg, 2012), and a final log2 ratio file in bedgraph format was generated. These files were visualized and analyzed by Integrative genomics viewer (IGV) (Robinson et al., 2011).

Quantification and statistical analysis

To quantify the hair-loss region in adult wing margin, mounted adult wings were imaged and the length of hair-loss regions was measured by QCapture Pro software (QImaging). For quantification of the intensity of GFP fluorescence in the wing disc, images were taken with the same confocal settings. The GFP fluorescence intensity of wing pouch region, posterior or anterior compartment of the wing pouch was measured using NIH ImageJ software.

Statistical analysis was performed using Graphpad Prism 8. For comparison between sample pairs, a two-tailed Student's *t*-test was used (Fig. 2G; Fig. 5A,B,E,J; Fig. S4M,N); for comparisons between three or more conditions, one-way ANOVA followed by Dunnett's multiple comparison tests were used (Fig. 1M,Q; Fig. 4L-R; Fig. 5N,R,V; Fig. S4L).

Acknowledgements

We thank Donna Arndt-Jovin, Andrea Brand, Peter Harte, Judith Kassis, Kenneth Irvine, Michelle Longworth, Jocelyn McDonald, Jürg Müller, Ying Su, Alain Vincent, Jian Wang, the Bloomington, DGRC, THFC and VDRC Stock Centers, and DSHB for fly stocks, antibodies and plasmids. We thank Dr Guilan Li at the National Center for Protein Science at Peking University for sample preparation, and Xinhan Meng and Di Yang in Zhu laboratory for assistance with ChIP and DamID analyses.

Competing interests

The authors declare no competing or financial interests.

Author contributions

Conceptualization: A.J.Z., T.H.; Methodology: T.H., Y.F.; Software: M.Y.; Validation: T.H.; Investigation: T.H., Y.F., J.D., Y.L.; Data curation: T.H., Y.F., J.D., Y.L.; Writing - original draft: A.J.Z., M.L., T.H.; Writing - review & editing: A.J.Z., M.L.; Supervision: A.J.Z.; Funding acquisition: A.J.Z., M.L.

Funding

This work was supported by the National Natural Science Foundation of China (31830058 and 31725019 to A.J.Z.; 32170716 to M.L.), by the National Key Research and Development Program of China (2021YFA0805800 to A.J.Z. and M.L.),by the Ministry of Education Key Laboratory of Cell Proliferation and Differentiation (to A.J.Z.),by the Peking-Tsinghua Joint Center for Life Sciences (to A.J.Z.) and by the Qidong-SLS Innovation Fund (to A.J.Z.).

Data availability

The DamID-seq data in this study has been deposited in GEO under accession number GSE208357.

Peer review history

The peer review history is available online at https://journals.biologists.com/dev/lookup/doi/10.1242/dev.201297.reviewer-comments.pdf.

References

Acharyya, S., Sharma, S. M., Cheng, A. S., Ladner, K. J., He, W., Kline, W., Wang, H., Ostrowski, M. C., Huang, T. H. and Guttridge, D. C. (2010). TNF inhibits Notch-1 in skeletal muscle cells by Ezh2 and DNA methylation mediated repression: implications in duchenne muscular dystrophy. *PLoS ONE* **5**, e12479. doi:10.1371/journal.pone.0012479

Ahmad, K. and Spens, A. E. (2019). Separate Polycomb response elements control chromatin state and activation of the *vestigial* gene. *PLoS Genet.* **15**, e1007877. doi:10.1371/journal.pgen.1007877

Anderson, J., Salzer, C. L. and Kumar, J. P. (2006). Regulation of the retinal determination gene *dachshund* in the embryonic head and developing eye of *Drosophila*. *Dev. Biol.* **297**, 536-549. doi:10.1016/j.ydbio.2006.05.004

Artavanis-Tsakonas, S. and Muskavitch, M. A. T. (2010). Notch: the past, the present, and the future. *Curr. Top. Dev. Biol.* **92**, 1-29. doi:10.1016/S0070-2153(10)92001-2

Aster, J. C., Pear, W. S. and Blacklow, S. C. (2017). The varied roles of Notch in cancer. *Annu. Rev. Pathol.* **12**, 245-275. doi:10.1146/annurev-pathol-052016-100127

Baonza, A. and Freeman, M. (2005). Control of cell proliferation in the *Drosophila* eye by Notch signaling. *Dev. Cell* **8**, 529-539. doi:10.1016/j.devcel.2005.01.019

Bauer, M., Trupke, J. and Ringrose, L. (2016). The quest for mammalian Polycomb response elements: are we there yet? *Chromosoma* **125**, 471-496. doi:10.1007/s00412-015-0539-4

Beira, J. V., Torres, J. and Paro, R. (2018). Signalling crosstalk during early tumorigenesis in the absence of Polycomb silencing. *PLoS Genet.* **14**, e1007187. doi:10.1371/journal.pgen.1007187

Bi, C.-L., Cheng, Q., Yan, L.-Y., Wu, H.-Y., Wang, Q., Wang, P., Cheng, L., Wang, R., Yang, L., Li, J. et al. (2022). A prominent gene activation role for C-terminal binding protein in mediating PcG/trxG proteins through Hox gene regulation. *Development* **149**, dev200153. doi:10.1242/dev.200153

Bourbon, H.-M., Gonzy-Treboul, G., Peronnet, F., Alin, M.-F., Ardourel, C., Benassayag, C., Cribbs, D., Deutsch, J., Ferrer, P., Haenlin, M. et al. (2002). A P-insertion screen identifying novel X-linked essential genes in *Drosophila*. *Mech. Dev.* **110**, 71-83. doi:10.1016/S0925-4773(01)00566-4

Bray, S. J. (2016). Notch signalling in context. *Nat. Rev. Mol. Cell. Biol.* **17**, 722-735. doi:10.1038/nrm.2016.94

Brennan, K., Tateson, R., Lieber, T., Couso, J. P., Zecchini, V. and Arias, A. M. (1999). The *abruptex* mutations of Notch disrupt the establishment of proneural clusters in *Drosophila*. *Dev. Biol.* **216**, 230-242. doi:10.1006/dbio.1999.9501

Brook, W. J. and Cohen, S. M. (1996). Antagonistic interactions between *wingless* and *decapentaplegic* responsible for dorsal-ventral pattern in the *Drosophila* leg. *Science* **273**, 1373-1377. doi:10.1126/science.273.5280.1373

Caussinus, E., Kanca, O. and Affolter, M. (2012). Fluorescent fusion protein knockout mediated by anti-GFP nanobody. *Nat. Struct. Mol. Biol.* **19**, 117-121. doi:10.1038/nsmb.2180

Chan, C. S., Rastelli, L. and Pirrotta, V. (1994). A Polycomb response element in the *Ubx* gene that determines an epigenetically inherited state of repression. *EMBO J.* **13**, 2553-2564. doi:10.1002/j.1460-2075.1994.tb06545.x

Classen, A.-K., Bunker, B. D., Harvey, K. F., Vaccari, T. and Bilder, D. (2009). A tumor suppressor activity of *Drosophila* Polycomb genes mediated by JAK-STAT signaling. *Nat. Genet.* **41**, 1150-1155. doi:10.1038/ng.445

Cohen, I., Zhao, D., Bar, C., Valdes, V. J., Dauber-Decker, K. L., Nguyen, M. B., Nakayama, M., Rendl, M., Bickmore, W. A., Koseki, H. et al. (2018). PRC1 fine-tunes gene repression and activation to safeguard skin development and stem cell specification. *Cell Stem Cell* **22**, 726-739.e7. doi:10.1016/j.stem.2018.04.005

Córdoba, S. and Estella, C. (2014). The bHLH-PAS transcription factor dysfusion regulates tarsal joint formation in response to Notch activity during *Drosophila* leg development. *PLoS Genet.* **10**, e1004621. doi:10.1371/journal.pgen.1004621

Cras-Méneur, C., Li, L., Kopan, R. and Permutt, M. A. (2009). Presenilins, Notch dose control the fate of pancreatic endocrine progenitors during a narrow developmental window. *Genes Dev.* **23**, 2088-2101. doi:10.1101/gad.1800209

Cuddapah, S., Roh, T.-Y., Cui, K., Jose, C. C., Fuller, M. T., Zhao, K. and Chen, X. (2012). A novel human polycomb binding site acts as a functional Polycomb response element in *Drosophila*. *PLoS ONE* **7**, e36365. doi:10.1371/journal.pone.0036365

Cunningham, M. D., Brown, J. L. and Kassis, J. A. (2010). Characterization of the Polycomb group response elements of the *Drosophila melanogaster invected* locus. *Mol. Cell. Biol.* **30**, 820-828. doi:10.1128/MCB.01287-09

De, S., Mitra, A., Cheng, Y., Pfeifer, K. and Kassis, J. A. (2016). Formation of a Polycomb-domain in the absence of strong Polycomb response elements. *PLoS Genet.* **12**, e1006200. doi:10.1371/journal.pgen.1006200

de Celis, J. F. and Bray, S. (1997). Feed-back mechanisms affecting Notch activation at the dorsoventral boundary in the *Drosophila* wing. *Development* **124**, 3241-3251. doi:10.1242/dev.124.17.3241

de Celis, J. F., Marí-Beffa, M. and García-Bellido, A. (1991). Cell-autonomous role of Notch, an epidermal growth factor homologue, in sensory organ differentiation in *Drosophila*. *Proc. Natl. Acad. Sci. USA* **88**, 632-636. doi:10.1073/pnas.88.2.632

de Celis, J. F., Barrio, R., del Arco, A. and García-Bellido, A. (1993). Genetic and molecular characterization of a *Notch* mutation in its Delta- and Serrate-binding domain in *Drosophila*. *Proc. Natl. Acad. Sci. USA* **90**, 4037-4041. doi:10.1073/pnas.90.9.4037

De Strooper, B., Annaert, W., Cupers, P., Saftig, P., Craessaerts, K., Mumm, J. S., Schroeter, E. H., Schrijvers, V., Wolfe, M. S., Ray, W. J. et al. (1999). A Presenilin-1-dependent γ-Secretase-like protease mediates release of Notch intracellular domain. *Nature* **398**, 518-522. doi:10.1038/19083

Déjardin, J., Rappailles, A., Cuvier, O., Grimaud, C., Decoville, M., Locker, D. and Cavalli, G. (2005). Recruitment of *Drosophila* Polycomb group proteins to chromatin by DSP1. *Nature* **434**, 533-538. doi:10.1038/nature03386

Dietzel, S., Niemann, H., Brückner, B., Maurange, C. and Paro, R. (1999). The nuclear distribution of Polycomb during *Drosophila melanogaster* development shown with a GFP fusion protein. *Chromosoma* **108**, 83-94. doi:10.1007/s004120050355

Dong, P. D. S., Chu, J. and Panganiban, G. (2001). Proximodistal domain specification and interactions in developing *Drosophila* appendages. *Development* **128**, 2365-2372. doi:10.1242/dev.128.12.2365

Du, J., Zhang, J., He, T., Li, Y., Su, Y., Tie, F., Liu, M., Harte, P. J. and Zhu, A. J. (2016). Stuxnet facilitates the degradation of Polycomb protein during development. *Dev. Cell* **37**, 507-519. doi:10.1016/j.devcel.2016.05.013

Evans, C. J., Liu, T. and Banerjee, U. (2014). *Drosophila* hematopoiesis: markers and methods for molecular genetic analysis. *Methods* **68**, 242-251. doi:10.1016/j.ymeth.2014.02.038

Felician, G., Collesi, C., Lusic, M., Martinelli, V., Ferro, M. D., Zentilin, L., Zacchigna, S. and Giacca, M. (2014). Epigenetic modification at Notch responsive promoters blunts efficacy of inducing notch pathway reactivation after myocardial infarction. *Circ. Res.* **115**, 636-649. doi:10.1161/CIRCRESAHA.115.304517

Félix, M.-A. and Wagner, A. (2008). Robustness and evolution: concepts, insights and challenges from a developmental model system. *Heredity* **100**, 132-140. doi:10.1038/sj.hdy.6800915

Feng, S., Huang, J. and Wang, J. (2011). Loss of the Polycomb group gene *polyhomeotic* induces non-autonomous cell overproliferation. *EMBO Rep.* **12**, 157-163. doi:10.1038/embor.2010.188

Ficz, G., Heintzmann, R. and Arndt-Jovin, D. J. (2005). Polycomb group protein complexes exchange rapidly in living *Drosophila*. *Development* **132**, 3963-3976. doi:10.1242/dev.01950

Foltz, D. R., Santiago, M. C., Berechid, B. E. and Nye, J. S. (2002). Glycogen synthase kinase-3β modulates Notch signaling and stability. *Curr. Biol.* **12**, 1006-1011. doi:10.1016/S0960-9822(02)00888-6

Fryer, C. J., White, J. B. and Jones, K. A. (2004). Mastermind recruits CycC:CDK8 to phosphorylate the Notch ICD and coordinate activation with turnover. *Mol. Cell* **16**, 509-520. doi:10.1016/j.molcel.2004.10.014

Gargiulo, G., Cesaroni, M., Serresi, M., de Vries, N., Hulsman, D., Bruggeman, S. W., Lancini, C. and van Lohuizen, M. (2013). *In vivo* RNAi screen for BMI1 targets identifies TGF-β/BMP-ER stress pathways as key regulators of neural- and malignant glioma-stem cell homeostasis. *Cancer Cell* **23**, 660-676. doi:10.1016/j.ccr.2013.03.030

Grossniklaus, U. and Paro, R. (2014). Transcriptional silencing by Polycomb-group proteins. *Cold Spring Harb. Perspect. Biol.* **6**, a019331. doi:10.1101/cshperspect.a019331

Guarani, V., Deflorian, G., Franco, C. A., Krüger, M., Phng, L.-K., Bentley, K., Toussaint, L., Dequiedt, F., Mostoslavsky, R., Schmidt, M. H. H. et al. (2011). Acetylation-dependent regulation of endothelial Notch signalling by the SIRT1 deacetylase. *Nature* **473**, 234-238. doi:10.1038/nature09917

Hartenstein, V. and Posakony, J. W. (1989). Development of adult sensilla on the wing and notum of *Drosophila melanogaster*. *Development* **107**, 389-405. doi:10.1242/dev.107.2.389

Hein, K., Mittler, G., Cizelsky, W., Kühl, M., Ferrante, F., Liefke, R., Berger, I. M., Just, S., Sträng, J. E., Kestler, H. A. et al. (2015). Site-specific methylation of Notch1 controls the amplitude and duration of the Notch1 response. *Sci. Signal.* **8**, ra30. doi:10.1126/scisignal.2005892

Henrique, D. and Schweisguth, F. (2019). Mechanisms of Notch signaling: a simple logic deployed in time and space. *Development* **146**, dev172148. doi:10.1242/dev.172148

Hori, K., Fostier, M., Ito, M., Fuwa, T. J., Go, M. J., Okano, H., Baron, M. and Matsuno, K. (2004). *Drosophila* Deltex mediates Suppressor of Hairless-independent and late-endosomal activation of Notch signaling. *Development* **131**, 5527-5537. doi:10.1242/dev.01448

Huang, F., Dambly-Chaudière, C. and Ghysen, A. (1991). The emergence of sense organs in the wing disc of *Drosophila*. *Development* **111**, 1087-1095. doi:10.1242/dev.111.4.1087

Jehn, B. M., Dittert, I., Beyer, S., von der Mark, K. and Bielke, W. (2002). c-Cbl binding and ubiquitin-dependent lysosomal degradation of membrane-associated Notch1. *J. Biol. Chem.* **277**, 8033-8040. doi:10.1074/jbc.M108552200

Jin, L., Vu, T., Yuan, G. and Datta, P. K. (2017). STRAP promotes stemness of human colorectal cancer via epigenetic regulation of the NOTCH pathway. *Cancer Res.* **77**, 5464-5478. doi:10.1158/0008-5472.CAN-17-0286

Jung, S.-H., Evans, C. J., Uemura, K. and Banerjee, U. (2005). The *Drosophila* lymph gland as a developmental model of hematopoiesis. *Development* **132**, 2521-2533. doi:10.1242/dev.01837

Kassis, J. A. (1994). Unusual properties of regulatory DNA from the *Drosophila engrailed* gene: three "pairing-sensitive" sites within a 1.6-kb region. *Genetics* **136**, 1025-1038. doi:10.1093/genetics/136.3.1025

Kassis, J. A., Kennison, J. A. and Tamkun, J. W. (2017). Polycomb and Trithorax group genes in *Drosophila*. *Genetics* **206**, 1699-1725. doi:10.1534/genetics.115.185116

Kopan, R. (1999). All good things must come to an end: how is Notch signaling turned off? *Sci. STKE* **1999**, PE1. doi:10.1126/scisignal.91999pe1

Koyama, D., Kikuchi, J., Hiraoka, N., Wada, T., Kurosawa, H., Chiba, S. and Furukawa, Y. (2014). Proteasome inhibitors exert cytotoxicity and increase chemosensitivity via transcriptional repression of Notch1 in T-cell acute lymphoblastic leukemia. *Leukemia* **28**, 1216-1226. doi:10.1038/leu.2013.366

Ku, H.-Y. and Sun, Y. H. (2017). Notch-dependent epithelial fold determines boundary formation between developmental fields in the *Drosophila* antenna. *PLoS Genet.* **13**, e1006898. doi:10.1371/journal.pgen.1006898

Lambertini, C., Pantano, S. and Dotto, G. P. (2010). Differential control of *Notch1* gene transcription by Klf4 and Sp3 transcription factors in normal versus cancer-derived keratinocytes. *PLoS ONE* **5**, e10369. doi:10.1371/journal.pone.0010369

Lan, W., Liu, S., Zhao, L. and Su, Y. (2020). Regulation of *Drosophila* hematopoiesis in lymph gland: from a developmental signaling point of view. *Int. J. Mol. Sci.* **21**, 5246. doi:10.3390/ijms21155246

Langlais, K. K., Brown, J. L. and Kassis, J. A. (2012). Polycomb group proteins bind an *engrailed* PRE in both the "ON" and "OFF" transcriptional states of *engrailed*. *PLoS ONE* **7**, e48765. doi:10.1371/journal.pone.0048765

Langmead, B. and Salzberg, S. L. (2012). Fast gapped-read alignment with Bowtie 2. *Nat. Methods* **9**, 357-359. doi:10.1038/nmeth.1923

Lebestky, T., Chang, T., Hartenstein, V. and Banerjee, U. (2000). Specification of *Drosophila* hematopoietic lineage by conserved transcription factors. *Science* **288**, 146-149. doi:10.1126/science.288.5463.146

Lebestky, T., Jung, S.-H. and Banerjee, U. (2003). A Serrate-expressing signaling center controls *Drosophila* hematopoiesis. *Genes Dev.* **17**, 348-353. doi:10.1101/gad.1052803

Lefort, K., Mandinova, A., Ostano, P., Kolev, V., Calpini, V., Kolfschoten, I., Devgan, V., Lieb, J., Raffoul, W., Hohl, D. et al. (2007). *Notch1* is a p53 target gene involved in human keratinocyte tumor suppression through negative regulation of ROCK1/2 and MRCKα kinases. *Genes Dev.* **21**, 562-577. doi:10.1101/gad.1484707

Li, N., Fassl, A., Chick, J., Inuzuka, H., Li, X., Mansour, M. R., Liu, L., Wang, H., King, B., Shaik, S. et al. (2014). Cyclin C is a haploinsufficient tumour suppressor. *Nat. Cell Biol.* **16**, 1080-1091. doi:10.1038/ncb3046

Loubiere, V., Delest, A., Thomas, A., Bonev, B., Schuettengruber, B., Sati, S., Martinez, A.-M. and Cavalli, G. (2016). Coordinate redeployment of PRC1 proteins suppresses tumor formation during *Drosophila* development. *Nat. Genet.* **48**, 1436-1442. doi:10.1038/ng.3671

Loubiere, V., Delest, A., Schuettengruber, B., Martinez, A.-M. and Cavalli, G. (2017). Chromatin immunoprecipitation experiments from whole *Drosophila*

embryos or larval imaginal discs. *Bio-Protocol* **7**, e2327. doi:10.21769/BioProtoc.2327

Marshall, O. J. and Brand, A. H. (2015). damidseq_pipeline: an automated pipeline for processing DamID sequencing datasets. *Bioinformatics (Oxford, England)* **31**, 3371-3373. doi:10.1093/bioinformatics/btv386

Martinez, A.-M., Schuettengruber, B., Sakr, S., Janic, A., Gonzalez, C. and Cavalli, G. (2009). Polyhomeotic has a tumor suppressor activity mediated by repression of Notch signaling. *Nat. Genet.* **41**, 1076-1082. doi:10.1038/ng.414

Mašek, J. and Andersson, E. R. (2017). The developmental biology of genetic Notch disorders. *Development* **144**, 1743-1763. doi:10.1242/dev.148007

McIntyre, B., Asahara, T. and Alev, C. (2020). Overview of basic mechanisms of Notch signaling in development and disease. *Adv. Exp. Med. Biol.* **1227**, 9-27. doi:10.1007/978-3-030-36422-9_2

Mihaly, J., Hogga, I., Gausz, J., Gyurkovics, H. and Karch, F. (1997). *In situ* dissection of the *Fab-7* region of the *bithorax* complex into a chromatin domain boundary and a Polycomb-response element. *Development* **124**, 1809-1820. doi:10.1242/dev.124.9.1809

Mo, J.-S., Kim, M.-Y., Han, S.-O., Kim, I.-S., Ann, E.-J., Lee, K. S., Seo, M.-S., Kim, J.-Y., Lee, S.-C., Park, J.-W. et al. (2007). Integrin-linked kinase controls Notch1 signaling by down-regulation of protein stability through Fbw7 ubiquitin ligase. *Mol. Cell. Biol.* **27**, 5565-5574. doi:10.1128/MCB.02372-06

Morey, L., Santanach, A., Blanco, E., Aloia, L., Nora, E. P., Bruneau, B. G. and Di Croce, L. (2015). Polycomb regulates mesoderm cell fate-specification in embryonic stem cells through activation and repression mechanisms. *Cell Stem Cell* **17**, 300-315. doi:10.1016/j.stem.2015.08.009

Mukherjee, A., Veraksa, A., Bauer, A., Rosse, C., Camonis, J. and Artavanis-Tsakonas, S. (2005). Regulation of Notch signalling by non-visual β-arrestin. *Nat. Cell Biol.* **7**, 1191-1201. doi:10.1038/ncb1327

Müller, J., Gaunt, S. and Lawrence, P. A. (1995). Function of the Polycomb protein is conserved in mice and flies. *Development* **121**, 2847-2852. doi:10.1242/dev.121.9.2847

Ogiyama, Y., Schuettengruber, B., Papadopoulos, G. L., Chang, J.-M. and Cavalli, G. (2018). Polycomb-dependent chromatin looping contributes to gene silencing during *Drosophila* development. *Mol. Cell* **71**, 73-88.e5. doi:10.1016/j.molcel.2018.05.032

Papayannopoulos, V., Tomlinson, A., Panin, V. M., Rauskolb, C. and Irvine, K. D. (1998). Dorsal-ventral signaling in the *Drosophila* eye. *Science* **281**, 2031-2034. doi:10.1126/science.281.5385.2031

Pherson, M., Misulovin, Z., Gause, M., Mihindukulasuriya, K., Swain, A. and Dorsett, D. (2017). Polycomb repressive complex 1 modifies transcription of active genes. *Sci. Adv.* **3**, e1700944. doi:10.1126/sciadv.1700944

Port, F., Chen, H.-M., Lee, T. and Bullock, S. L. (2014). Optimized CRISPR/Cas tools for efficient germline and somatic genome engineering in *Drosophila*. *Proc. Natl. Acad. Sci. USA* **111**, E2967-E2976. doi:10.1073/pnas.1405500111

Qiu, L., Joazeiro, C., Fang, N., Wang, H.-Y., Elly, C., Altman, Y., Fang, D., Hunter, T. and Liu, Y.-C. (2000). Recognition and ubiquitination of Notch by Itch, a HECT-type E3 ubiquitin ligase. *J. Biol. Chem.* **275**, 35734-35737. doi:10.1074/jbc.M007300200

Robinson, J. T., Thorvaldsdóttir, H., Winckler, W., Guttman, M., Lander, E. S., Getz, G. and Mesirov, J. P. (2011). Integrative genomics viewer. *Nat. Biotechnol.* **29**, 24-26. doi:10.1038/nbt.1754

Saj, A., Arziman, Z., Stempfle, D., van Belle, W., Sauder, U., Horn, T., Dürrenberger, M., Paro, R., Boutros, M. and Merdes, G. (2010). A combined *ex vivo* and *in vivo* RNAi screen for Notch regulators in *Drosophila* reveals an extensive Notch interaction network. *Dev. Cell* **18**, 862-876. doi:10.1016/j.devcel.2010.03.013

Sakata, T., Sakaguchi, H., Tsuda, L., Higashitani, A., Aigaki, T., Matsuno, K. and Hayashi, S. (2004). *Drosophila* Nedd4 regulates endocytosis of Notch and suppresses its ligand-independent activation. *Curr. Biol.* **14**, 2228-2236. doi:10.1016/j.cub.2004.12.028

Sasamura, T., Ishikawa, H. O., Sasaki, N., Higashi, S., Kanai, M., Nakao, S., Ayukawa, T., Aigaki, T., Noda, K., Miyoshi, E. et al. (2007). The O-fucosyltransferase O-fut1 is an extracellular component that is essential for the constitutive endocytic trafficking of Notch in *Drosophila*. *Development* **134**, 1347-1356. doi:10.1242/dev.02811

Schuettengruber, B., Ganapathi, M., Leblanc, B., Portoso, M., Jaschek, R., Tolhuis, B., van Lohuizen, M., Tanay, A. and Cavalli, G. (2009). Functional anatomy of Polycomb and Trithorax chromatin landscapes in *Drosophila* embryos. *PLoS Biol.* **7**, e13. doi:10.1371/journal.pbio.1000013

Schuettengruber, B., Bourbon, H.-M., Di Croce, L. and Cavalli, G. (2017). Genome regulation by Polycomb and Trithorax: 70 years and counting. *Cell* **171**, 34-57. doi:10.1016/j.cell.2017.08.002

Schwanbeck, R. (2015). The role of epigenetic mechanisms in Notch signaling during development. *J. Cell Physiol.* **230**, 969-981. doi:10.1002/jcp.24851

Sengupta, A. K., Kuhrs, A. and Müller, J. (2004). General transcriptional silencing by a Polycomb response element in *Drosophila*. *Development* **131**, 1959-1965. doi:10.1242/dev.01084

Shen, W. and Mardon, G. (1997). Ectopic eye development in *Drosophila* induced by directed *dachshund* expression. *Development* **124**, 45-52. doi:10.1242/dev.124.1.45

Simon, J., Chiang, A., Bender, W., Shimell, M. J. and O'Connor, M. (1993). Elements of the *Drosophila bithorax* complex that mediate repression by Polycomb group products. *Dev. Biol.* **158**, 131-144. doi:10.1006/dbio.1993.1174

Sipos, L., Kozma, G., Molnár, E. and Bender, W. (2007). *In situ* dissection of a Polycomb response element in *Drosophila melanogaster*. *Proc. Natl. Acad. Sci. USA* **104**, 12416-12421. doi:10.1073/pnas.0703144104

Sjöqvist, M., Antfolk, D., Ferraris, S., Rraklli, V., Haga, C., Antila, C., Mutvei, A., Imanishi, S. Y., Holmberg, J., Jin, S. et al. (2014). PKCζ regulates Notch receptor routing and activity in a Notch signaling-dependent manner. *Cell Res.* **24**, 433-450. doi:10.1038/cr.2014.34

Southall, T. D., Davidson, C. M., Miller, C., Carr, A. and Brand, A. H. (2014). Dedifferentiation of neurons precedes tumor formation in *Lola* mutants. *Dev. Cell* **28**, 685-696. doi:10.1016/j.devcel.2014.01.030

Spatz, L. B., Jin, R. U. and Mills, J. C. (2021). Cellular plasticity at the nexus of development and disease. *Development* **148**, dev197392. doi:10.1242/dev.197392

Sprinzak, D. and Blacklow, S. C. (2021). Biophysics of Notch signaling. *Annu. Rev. Biophys.* **50**, 157-189. doi:10.1146/annurev-biophys-101920-082204

Steffen, P. A. and Ringrose, L. (2014). What are memories made of? How Polycomb and Trithorax proteins mediate epigenetic memory. *Nat. Rev. Mol. Cell Biol.* **15**, 340-356. doi:10.1038/nrm3789

Stern, C. D. (2022). Reflections on the past, present and future of developmental biology. *Dev. Biol.* **488**, 30-34. doi:10.1016/j.ydbio.2022.05.001

Struhl, G. and Greenwald, I. (1999). Presenilin is required for activity and nuclear access of Notch in *Drosophila*. *Nature* **398**, 522-525. doi:10.1038/19091

Su, Y., Ospina, J. K., Zhang, J., Michelson, A. P., Schoen, A. M. and Zhu, A. J. (2011). Sequential phosphorylation of Smoothened transduces graded Hedgehog signaling. *Sci. Signal.* **4**, ra43. doi:10.1126/scisignal.2001747

Taranova, O. V., Magness, S. T., Fagan, B. M., Wu, Y., Surzenko, N., Hutton, S. R. and Pevny, L. H. (2006). SOX2 is a dose-dependent regulator of retinal neural progenitor competence. *Genes Dev.* **20**, 1187-1202. doi:10.1101/gad.1407906

Toba, G., Ohsako, T., Miyata, N., Ohtsuka, T., Seong, K.-H. and Aigaki, T. (1999). The gene search system: a method for efficient detection and rapid molecular identification of genes in *Drosophila melanogaster*. *Genetics* **151**, 725-737. doi:10.1093/genetics/151.2.725

Torres, J., Monti, R., Moore, A. L., Seimiya, M., Jiang, Y., Beerenwinkel, N., Beisel, C., Beira, J. V. and Paro, R. (2018). A switch in transcription and cell fate governs the onset of an epigenetically-deregulated tumor in *Drosophila*. *eLife* **7**, e32697. doi:10.7554/eLife.32697

Vogel, M. J., Peric-Hupkes, D. and van Steensel, B. (2007). Detection of *in vivo* protein-DNA interactions using DamID in mammalian cells. *Nat. Protoc.* **2**, 1467-1478. doi:10.1038/nprot.2007.148

Wang, J., Xu, S.-L., Duan, J.-J., Yi, L., Guo, Y.-F., Shi, Y., Li, L., Yang, Z.-Y., Liao, X.-M., Cai, J. et al. (2019). Invasion of white matter tracts by glioma stem cells is regulated by a NOTCH1-SOX2 positive-feedback loop. *Nat. Neurosci.* **22**, 91-105. doi:10.1038/s41593-018-0285-z

Wilkin, M. B., Carbery, A.-M., Fostier, M., Aslam, H., Mazaleyrat, S. L., Higgs, J., Myat, A., Evans, D. A. P., Cornell, M. and Baron, M. (2004). Regulation of Notch endosomal sorting and signaling by *Drosophila* Nedd4 family proteins. *Curr. Biol.* **14**, 2237-2244. doi:10.1016/j.cub.2004.11.030

Wu, G., Lyapina, S., Das, I., Li, J., Gurney, M., Pauley, A., Chui, I., Deshaies, R. J. and Kitajewski, J. (2001). SEL-10 is an inhibitor of Notch signaling that targets Notch for ubiquitin-mediated protein degradation. *Mol. Cell. Biol.* **21**, 7403-7415. doi:10.1128/MCB.21.21.7403-7415.2001

Wu, J., Iwata, F., Grass, J. A., Osborne, C. S., Elnitski, L., Fraser, P., Ohneda, O., Yamamoto, M. and Bresnick, E. H. (2005). Molecular determinants of *NOTCH4* transcription in vascular endothelium. *Mol. Cell. Biol.* **25**, 1458-1474. doi:10.1128/MCB.25.4.1458-1474.2005

Xiao, L., Fan, D., Qi, H., Cong, Y. and Du, Z. (2022). Defect-buffering cellular plasticity increases robustness of metazoan embryogenesis. *Cell Syst.* **13**, 615-630.e9. doi:10.1016/j.cels.2022.07.001

Xu, T., Rebay, I., Fleming, R. J., Scottgale, T. N. and Artavanis-Tsakonas, S. (1990). The *Notch* locus and the genetic circuitry involved in early *Drosophila* neurogenesis. *Genes Dev.* **4**, 464-475. doi:10.1101/gad.4.3.464

Zhu, A. J., Zheng, L., Suyama, K. and Scott, M. P. (2003). Altered localization of *Drosophila* Smoothened protein activates Hedgehog signal transduction. *Genes Dev.* **17**, 1240-1252. doi:10.1101/gad.1080803

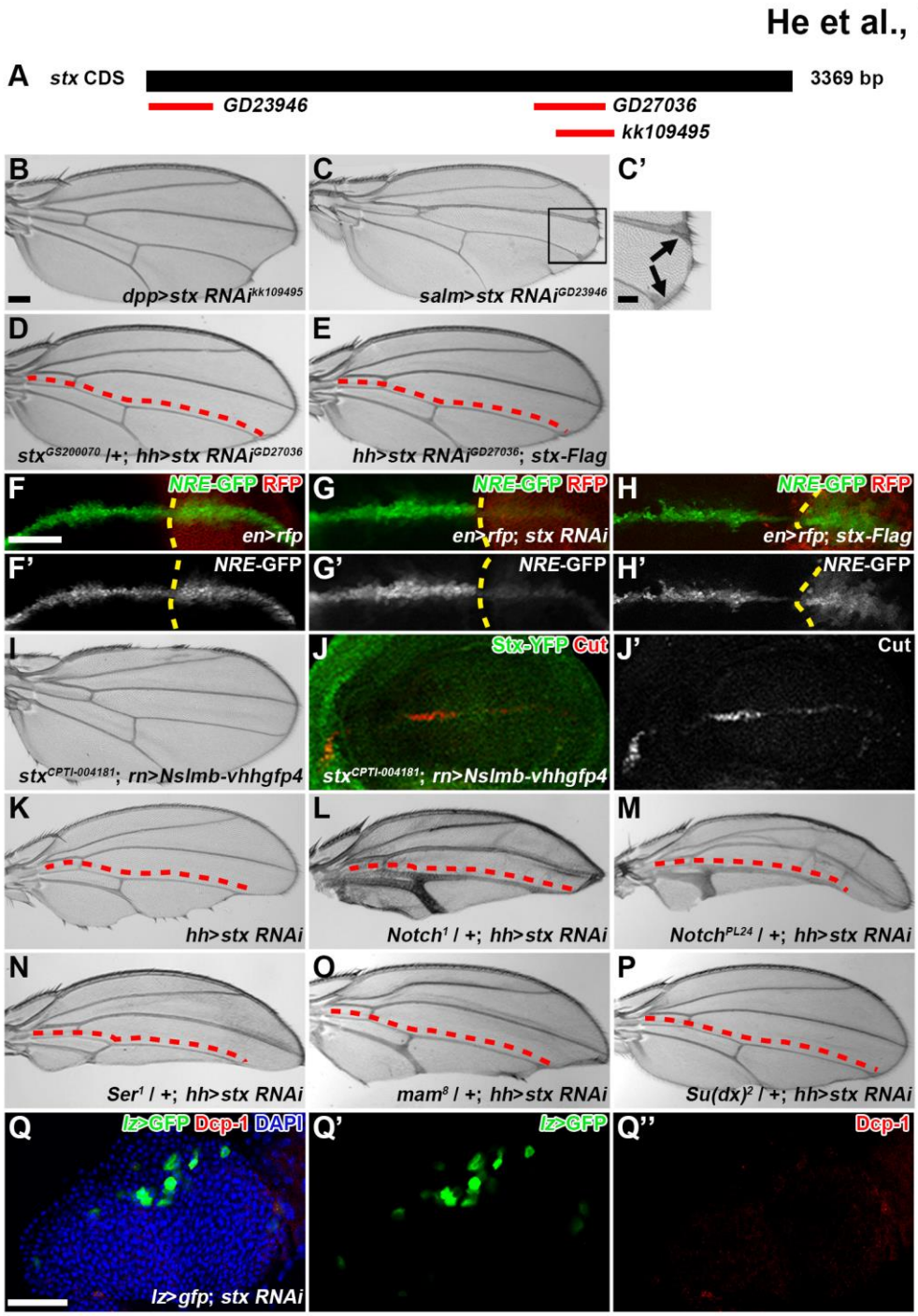

Fig. S1. *stx* positively regulates Notch signaling.

(A) Schematic diagram showing the targeted regions of three *stx* RNAi transgenic lines on the *stx* coding sequence. (B-E) Adult wings of the indicated genotype are shown. Knockdown of *stx* by two additional RNAi lines targeting different coding regions of *stx* resulted in similar wing notching phenotypes (B and C). The magnified box area in panel C is shown (C'); arrows mark small deltas distal to the L3 and L4 longitudinal veins. Overexpression of *stx* using a GS line (D) or a UAS-*stx*-*Flag* transgene (E) largely rescued the notched wing phenotype associated with *stx* RNAi.

(F-H') *NRE*-GFP reporter expression in wing discs of the indicated genotype is shown. Reducing *stx* expression by RNAi decreased *NRE*-GFP expression (G'; cf. F'), while overexpression of *stx* increased *NRE*-GFP activity (H'; cf. F').
(I-J') Adult wing and expression of Stx-YFP and Cut in wing discs of the indicated genotype are shown. Knockdown of *stx* by the deGradFP strategy in a CPTI line, in which a YFP protein trap cassette was inserted into the *stx* locus, resulted in a notched adult wing phenotype (I) and downregulation of Cut expression (J') in the wing disc.
(K-P) Adult wings of the indicated genotype are shown. When one copy of *Notch* (L, M), *Ser* (N) or *mam* (O) was mutated, the loss of wing margin tissue caused by *stx* RNAi (K) was exacerbated. In contrast, this phenotype was partially rescued in *Su(dx)*^{1} heterozygotes (P).
(Q-Q'') The expression of *lz*>GFP and cleaved Dcp-1 in the lymph gland of the indicated genotype is shown. Knocking down *stx* did not induce the cleavage of Dcp-1 in GFP-marked crystal cells.
The adult wings in are shown proximal to the left, with anterior/posterior (a/p) boundaries marked with red dashed lines. The wing discs are shown anterior to the left and ventral at the top, with a/p boundaries marked with yellow dashed lines.
Scale bar, B-E, I and K-P, 100 μm; C', F-H', J, J' and Q-Q'', 50 μm.

He et al., Figure S2

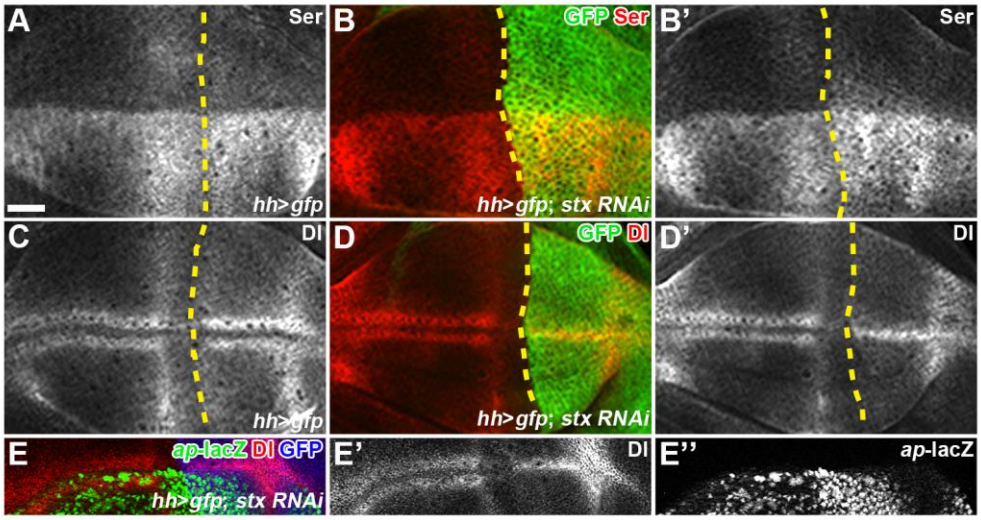

Fig. S2. *stx* does not regulate Dl or Ser expression.

Ser (A-B'), Dl (C-E'), and *ap*-lacZ expression (E, E') in the wing disc of the indicated genotype are shown. In GFP-marked posterior compartment cells where *stx* expression was knocked down by *hh*-Gal4-driven RNAi, Ser protein expression was unaffected (B'; cf. A), but the expression pattern of Dl changed from two stripes (C) to one stripe along the dorsal/ventral (D/V) boundary (D' and E-E''). The dorsal compartment of the wing disc was marked with *ap*-lacZ (E'').

The wing discs are shown anterior to the left and ventral at the top, with a/p boundaries marked with yellow dashed lines.

Scale bar, 50 μm.

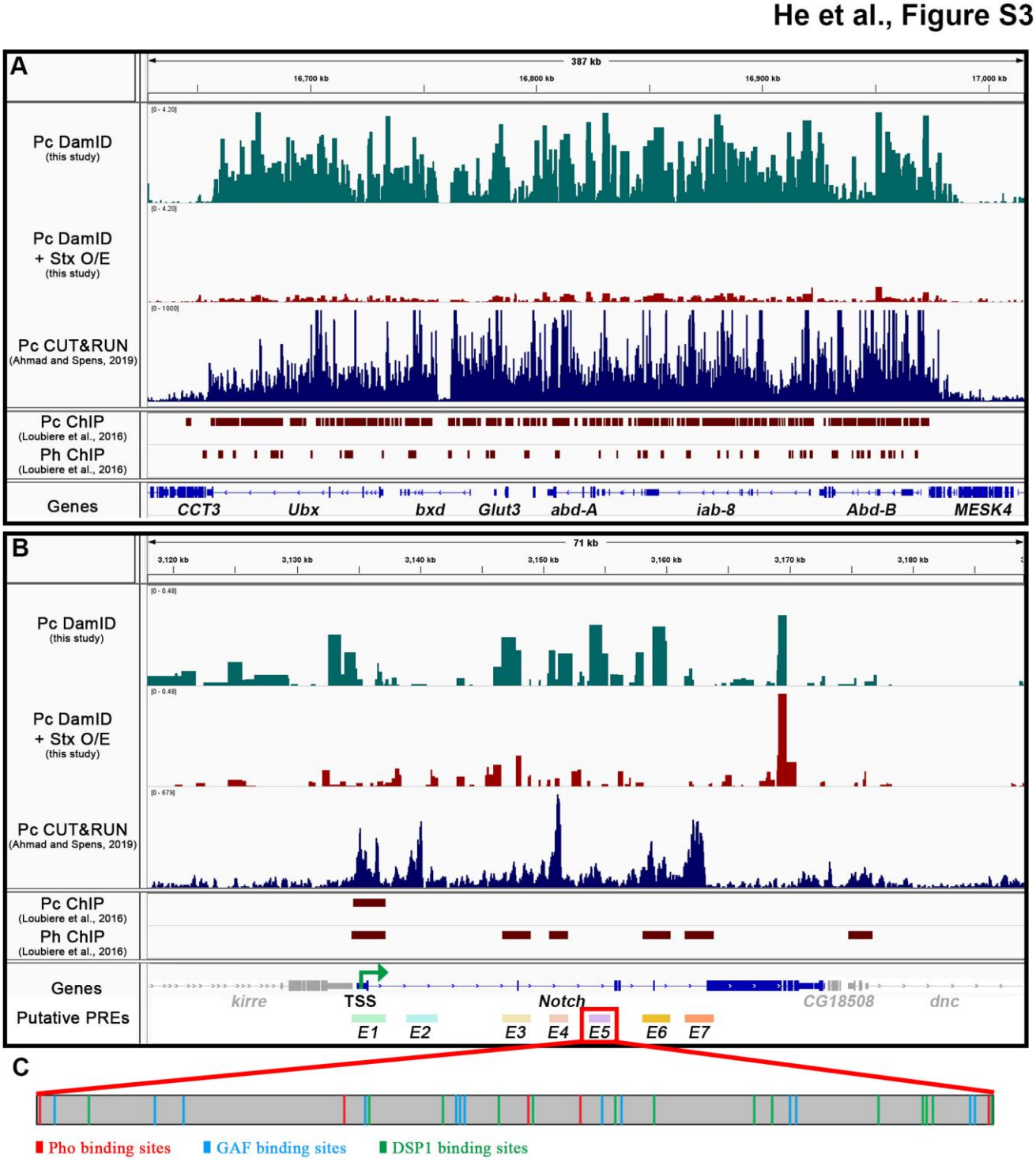

Fig. S3. Pc and Ph recruitment in canonical PcG target genes and the *Notch* locus.

(A) Pc and Ph recruitment to the indicated region containing canonical PcG target genes were compared by analysing three datasets: CUT&RUN and ChIP-seq data from the wing disc in previous studies (Loubiere et al., 2016; Ahmad and Spens, 2019) and the DamID-seq data generated in this study.

(B) Pc and Ph recruitment at the *Notch* locus were compared by analysing three datasets, as shown in A. The putative PREs are displayed as color-coded rectangles that match the PRE GFP reporter activity shown in Figure 4L, M and Figure S4L-N.

(C) Shown are the putative binding sites of Pho, GAGA, and DSP1 in the *E5* region.

He et al., Figure S4

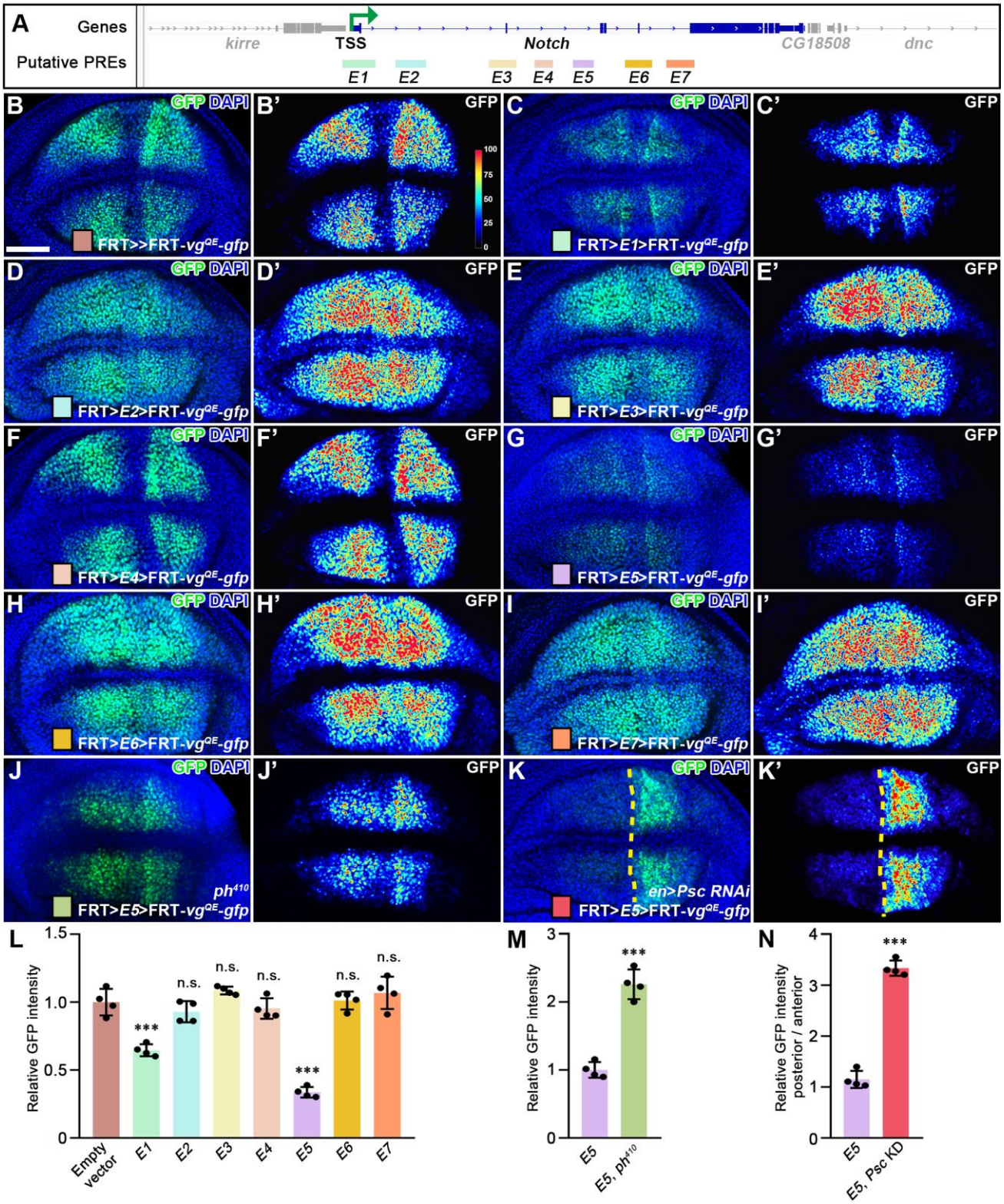

Fig. S4. *E1* and *E5* are potential functional PREs.

(A) Schematic diagram of the putative PREs (rectangles) in the *Notch* locus where each putative PRE is assigned a unique color key that matches the PRE GFP reporter activity shown in panels L-N.

(B-N) GFP reporter expression (B-K) and corresponding heatmap images (B'-K') of relative GFP intensity in wing discs of the indicated genotype are shown. The vertical color bar on the right (B') represents the intensity range. Both *E1* (C') and *E5* (G') were able to repress the expression of GFP reporter, with E5 showing a stronger effect, while the other five fragments had no inhibitory effects on GFP reporter expression (D', E', F', H', I'). Moreover, GFP expression of the *E5* reporter was significantly increased in loss-of-function ph^{410} mutant wing disc (J'; cf. G') and in the posterior compartment of the wing disc where *Psc* was knocked down by *en*-Gal4-driven RNAi (K'; cf. G'). Statistical analyses of relative GFP fluorescence intensity in wing discs of the indicated genotype (n=4) are shown (L-N). GFP activity controlled only by vg^{QE} was used as a normalized standard. Data were presented as mean±S.D, *** $p<0.001$, n.s. $p>0.05$ (One-way ANOVA, Dunnett's multiple comparison tests).

The wing discs are shown anterior to the left and ventral at the top, with a/p boundaries marked with yellow dashed lines.

Scale bar, 50 μm.

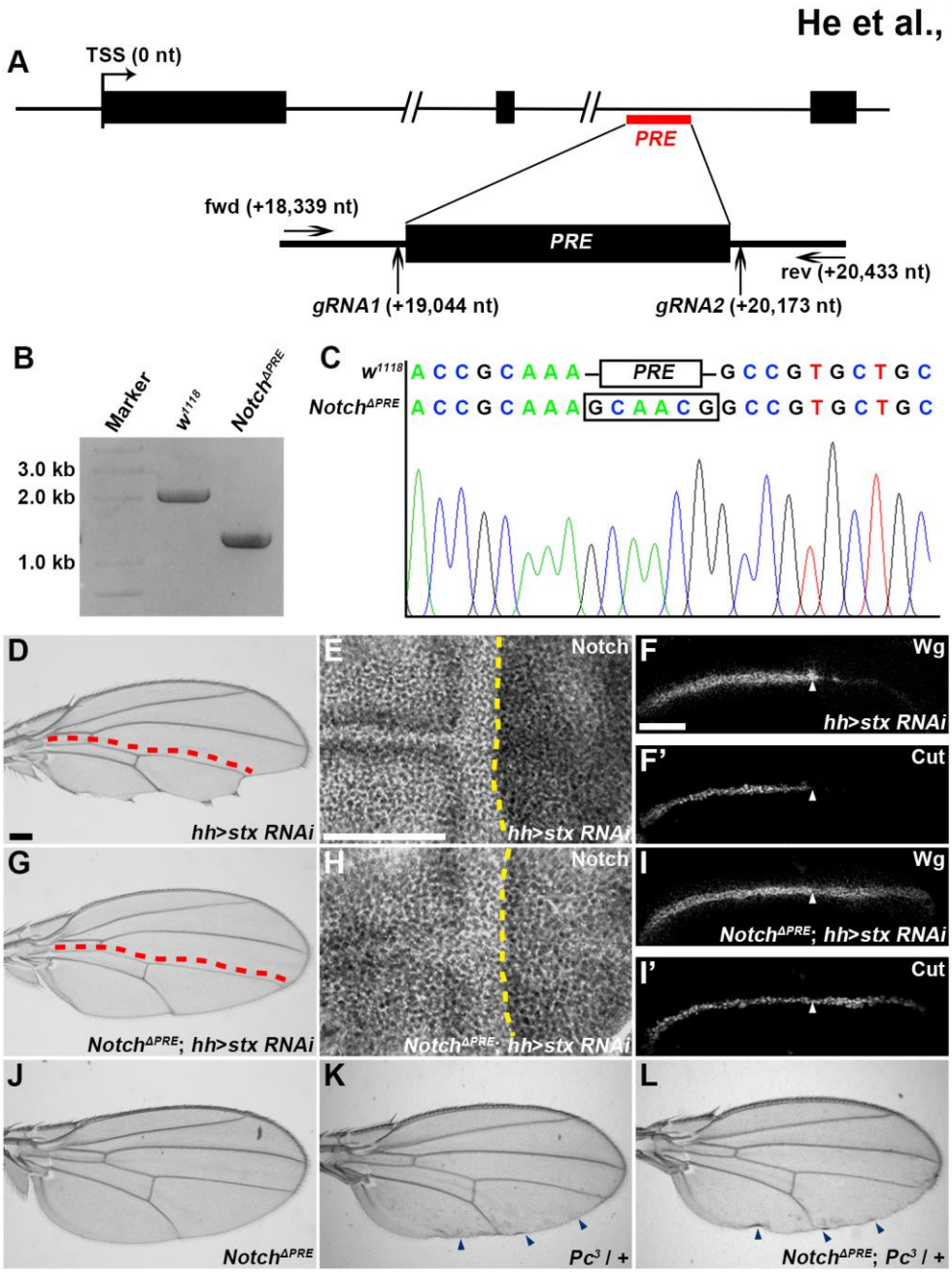

Fig. S5. The expression of Notch in *Notch*$^{\Delta PRE}$ mutant flies is no longer modulated by Stx and Pc.

(A) Schematic diagram showing the location of gRNAs and primers used to generate and validate the *Notch*$^{\Delta PRE}$ allele. (B) Using the forward and reverse primers shown in panel A, PCR products amplified using genomic DNA extracted from w^{1118} and *Notch*$^{\Delta PRE}$ flies, respectively, showed that the 1.1 Kb PRE sequence was removed from the *Notch* locus. (C) A comparison of the Sanger sequencing results of the two PCR products in panel B confirmed that the PRE sequence was deleted *in situ* from the *Notch*$^{\Delta PRE}$ allele.

(D-I') Adult wings (D, G) and the expression of Notch (E, H) and Notch signaling target genes Wg (F, I) and Cut (F', I') in the wing disc of the indicated genotype are shown. Knockdown of *stx* resulted in a notched adult wing phenotype (D) and downregulation of Notch (E), Wg (F), and Cut expression (F') in the wing disc. These phenotypes were largely restored in the $Notch^{\Delta PRE}$ mutant wing blade (G; cf. D) and wing discs (H-I'; cf. E-F'). The arrowhead marks the a/p boundary of the wing disc (F, F', I, I').

(J-L) Adult wings of the indicated genotype are shown. No apparent wing vein phenotype associated with gain-of-function Notch signaling was observed in adult $Notch^{\Delta PRE}$ wings (J), nor did Pc^{3} heterozygosity change this phenotype (L). Note that the posterior wing margin curvature phenotype of the Pc^{3} heterzygous wing (arrowheads in K and L) is due to partial transformation of the methothoracic wing to the metathoracic haltere (Bi et al., 2022), which is not related to Notch signaling alteration.

The adult wings are shown proximal to the left, with a/p boundaries marked with red dashed lines. The wing discs are shown anterior to the left and ventral at the top, with a/p boundaries marked with yellow dashed lines.

Scale bar, D, G and J-L, 100 μm; E-F' and H-I', 50 μm.

He et al., Figure S6

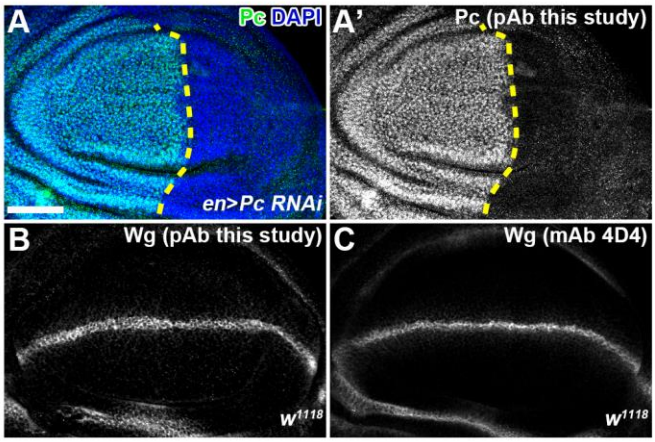

Fig. S6. Validation of the Pc and Wg antibodies generated in this study.

Pc (A, A') and Wg expression (B, C) in the wing disc of the indicated genotype were detected by the indicated antibodies. In posterior compartment cells where *Pc* expression was knocked down by *en*-Gal4-driven RNAi, the expression of Pc protein detected by the rabbit anti-Pc antibody generated in this study was significantly reduced (A'). Rabbit anti-Wg antibody (B) generated in this study and mouse anti-Wg antibody (C) purchased from DSHB (clone 4D4) detected similar Wg expression patterns in the wing pouch.

Wing discs are shown with anterior to the left and ventral at the top, with a/p boundaries marked with yellow dashed lines.

Scale bar, 50 μm.

Table S1. Genetic crosses for figures and supplemental figures

Click here to download Table S1

Table S2. List of primers used in this study

Click here to download Table S2